# Fluctuation spectroscopy of disordered two-dimensional superconductors

A. Glatz,[1] A. A. Varlamov,[1,2] and V. M. Vinokur[1]

[1]*Materials Science Division, Argonne National Laboratory, 9700 South Cass Avenue, Argonne, Illinois 60637, USA*

[2]*CNR-SPIN, Viale del Politecnico 1, I-00133 Rome, Italy*

(Received 7 December 2010; revised manuscript received 24 May 2011; published 12 September 2011)

We revise the long-studied problem of fluctuation conductivity (FC) in disordered two-dimensional superconductors placed in a perpendicular magnetic field by finally deriving the complete solution in the temperature-magnetic field phase diagram. The obtained expressions allow both to perform straightforward (numerical) calculation of the FC surface $\delta\sigma_{xx}^{(\mathrm{tot})}(T,H)$ and to get asymptotic expressions in all its qualitatively different domains. This surface becomes in particular nontrivial at low temperatures, where it is trough-shaped with $\delta\sigma_{xx}^{(\mathrm{tot})}(T,H)<0$. In this region, close to the quantum-phase transition, $\delta\sigma_{xx}^{(\mathrm{tot})}(T,H=\mathrm{const})$ is nonmonotonic, in agreement with experimental findings. We reanalyzed and present comparisons to several experimental measurements. Based on our results we derive a qualitative picture of superconducting fluctuations close to $H_{c2}(0)$ and $T=0$ where fluctuation Cooper pairs rotate with cyclotron frequency $\omega_c\sim\Delta_{\mathrm{BCS}}^{-1}$ and Larmor radius $\sim\xi_{\mathrm{BCS}}$, forming some kind of quantum liquid with long coherence length $\xi_{\mathrm{QF}}\gg\xi_{\mathrm{BCS}}$ and slow relaxation ($\tau_{\mathrm{QF}}\gg\hbar\Delta_{\mathrm{BCS}}^{-1}$).

DOI: 10.1103/PhysRevB.84.104510 PACS number(s): 74.40.−n

## I. INTRODUCTION

The understanding of the mechanisms of superconducting fluctuations (SFs), achieved during the past decades[1] provided a unique tool for obtaining information about the microscopic parameters of superconductors (SCs). SFs are composed of Cooper pairs with finite lifetime which appear already above the transition but do not form a stable condensate yet. They affect thermodynamic and transport properties of the normal state both directly and through the changes which they cause in the normal quasiparticle subsystem.[1]

SFs are commonly described in terms of three principal contributions: the Aslamazov-Larkin (AL) process, corresponding to the opening of a new channel for the charge transfer,[2] the anomalous Maki-Thompson (MT) process, which describes single-particle quantum interference at impurities in the presence of SFs,[3,4] and the change of the single-particle density of states (DOS) due to their involvement in fluctuation pairings.[5,6] The first two processes (AL and MT) result in the appearance of positive and singular contributions to conductivity (diagrams 1 and 2 in Fig. 1) close to the superconducting critical temperature $T_{c0}$, while the third one (DOS) results in a decrease of the Drude conductivity due to the lack of single-particle excitations at the Fermi level (diagrams 3–6 in Fig. 1). The latter contribution is less singular in temperature than the first two and can compete with them only if the AL and MT processes are suppressed for some reasons (for example, $c$-axis transport in layered SCs) or far away from $T_{c0}$.

The classical results obtained first in the vicinity of $T_{c0}$ were later generalized to temperatures far from the transition, for example, in Refs. 7–9, and to relatively high fields (see Ref. 10). More recently, quantum fluctuations (QFs) came into the focus of investigations. In Refs. 11 and 12 it was found that in granular SCs at very low temperatures and close to $H_{c2}(0)$, the positive AL contribution to magnetoconductivity decays as $T^2$ while the fluctuation suppression of the DOS results in a temperature-independent negative contribution, logaritmically growing in magnitude for $H\to H_{c2}(0)$. The authors of Ref. 13 came to the same conclusion while studying the effect of QFs on the Nernst-Ettingshausen coefficient in two-dimensional (2D) SCs. For the first time they attracted the attention[14] to the special role of diagrams 9 and 10 in Fig. 1.

In Ref. 15 the effects of QFs on magnetoconductivity and magnetization of 2D SCs were studied. The authors of this work analyzed all ten diagrams shown in Fig. 1 in the lowest Landau level (LLL) approximation, valid at fields close to the critical line $H_{c2}(T)$. They found a nontrivial nonmonotonic temperature behavior of the fluctuation magnetoconductivity at fields close to $H_{c2}(0)$ and demonstrated that, analogously to the situation in granular SCs, close to zero temperature, the fluctuation contribution is negative; that is, QFs increase resistivity and not conductivity (in contrast to the situation close to $T_{c0}$).

Yet the confidence in the exotic nature of negative fluctuation corrections and the common belief of fluctuation contributions to conductivity being positive beyond the narrow domain of the quantum-phase transition has been persistent and is based on available asymptotic expressions only. The region near $T=0$ and magnetic fields near $H_{c2}(0)$ remain poorly understood and, in addition, a universal picture combining QFs at high magnetic fields and conventional finite-temperature quantum corrections is still lacking.

This is why we revisit the problem of fluctuation conductivity of a disordered 2D superconductor placed in a perpendicular magnetic field in this paper.[16] We present an exact calculation (*without the use of the LLL approximation*) of all ten diagrams of the first order of fluctuation theory (see Fig. 1) valid in the whole $H$-$T$ phase diagram beyond the superconducting region, that is, for arbitrary fields $H\geqslant H_{c2}(T)$ and temperatures $T_c(H)\leqslant T$. The obtained expressions allow both to perform straightforward (numerical) calculations of the fluctuation conductivity "surface" $\delta\sigma_{xx}^{(\mathrm{tot})}(T,H)$ and to get asymptotic expressions in all of its qualitatively different domains.

 

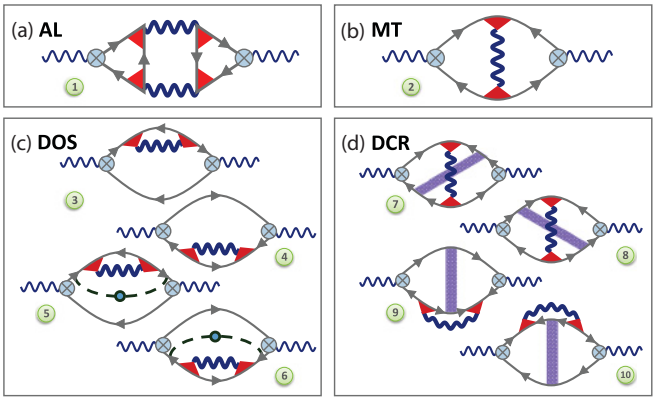


FIG. 1. (Color online) Feynman diagrams for the leading-order contributions to the electromagnetic response operator. Wavy lines stand for fluctuation propagators, solid lines with arrows are impurity-averaged normal state Green's functions, crossed circles are electric-field vertices, dashed lines with a circle represent additional impurity renormalizations, and triangles and dotted rectangles are impurity ladders accounting for the electron scattering at impurities (Cooperons).

A typical example of the surface $\delta\sigma_{xx}^{(\mathrm{tot})}(T,H)$ is presented in Fig. 2 and demonstrates that our revision and completion of the commonly believed understanding of fluctuation corrections is urgently called for: Its striking feature consists of the fact that the FC is positive only in the domain bound by the separatrices $H_{c2}(T)$ and $\delta\sigma_{xx}^{(\mathrm{tot})}(T,H)=0$ and is negative throughout all other parts of the phase diagram (see Fig. 3, in which the domains of different overall signs of $\delta\sigma_{xx}^{(\mathrm{tot})}(T,H)$ and contours of constant $\delta\sigma_{xx}^{(\mathrm{tot})}$ in the whole phase diagram are shown). Contrary to the common assumption, the FC is only positive in the domain of weak fields and temperatures above $T_{c0}$, the region of positive corrections depends on the magnitude of the positive anomalous MT contribution (i.e., on the value of the phase-breaking time $\tau_\phi$). With increasing magnetic field, the interval of temperatures where $\delta\sigma_{xx}^{(\mathrm{tot})}(T,H)>0$ shrinks and becomes zero close to $H_{c2}(0)$. In particular at low

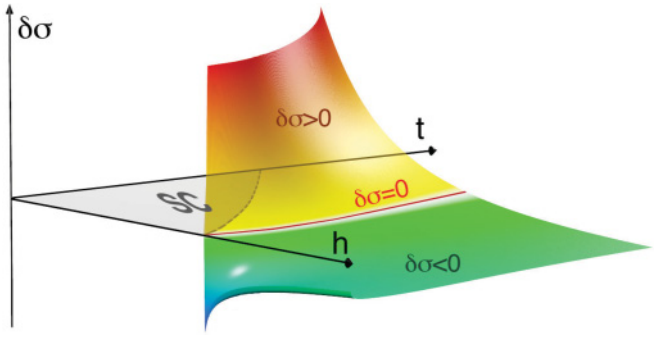


FIG. 2. (Color online) Fluctuation correction to conductivity (FC) $\delta\sigma=\delta\sigma_{xx}^{(\mathrm{tot})}(t,h)$ as a function of the reduced temperature $t=T/T_{c0}$ and magnetic field $h=0.69H/H_{c2}(0)$ plotted as surface. The FC changes its sign along the thick red line ($\delta\sigma=0$). The boundary of the superconducting region is shown by a dashed line. Here $\delta\sigma$ is plotted for constant $\tau T_{c0}=10^{-2}$ and $\tau_\phi T_{c0}=10$.

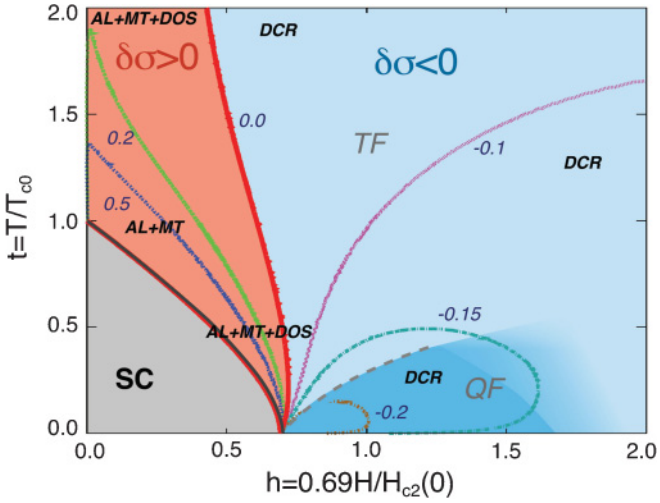


FIG. 3. (Color online) Contours of constant fluctuation conductivity [$\delta\sigma=\delta\sigma_{xx}^{(\mathrm{tot})}(t,h)$ shown in units of $e^2$]. The dominant FC contributions are indicated by bold-italic labels. The dashed line separates the domain of quantum fluctuations (QF) [dark area of $\delta\sigma<0$] and thermal fluctuations (TF). The contour lines are obtained from Eq. (5) with $T_{c0}\tau=0.01$ and $T_{c0}\tau_\phi=10$.

temperatures, the behavior of the FC turns out to be highly nontrivial. In this case, the surface $\delta\sigma_{xx}^{(\mathrm{tot})}(T,H)$ has a trough-shaped character and the dependence $\delta\sigma_{xx}^{(\mathrm{tot})}(T,H=\mathrm{const})$ is nonmonotonic. We see below that this feature is observed in available experimental results as well.

Our analysis also elucidates the understanding of the hierarchy of the various contributions to the fluctuation corrections in different domains of the phase diagram (see Fig. 3 in which the dominating fluctuation contributions to magnetoconductivity are indicated for different regions of the phase diagram). We demonstrate that the main fluctuation contributions close to $T_{c0}$, paraconductivity (AL), anomalous MT, and DOS, in the region of QF become zero as $\sim T^2$ (compare to Refs. 11,12, and 17). It is the fourth, usually ignored, fluctuation contribution, formally determined by the sum of diagrams 7–10 and the regular part of the MT diagram, which governs the quantum-phase transition (QPT). It can be identified by the renormalization of the single-particle diffusion coefficient in the presence of fluctuations (DCR) and it turns out that this contribution dominates in the periphery of the phase diagram including the vicinity of the QPT $[t=T/T_{c0}\ll\widetilde{h}=[H-H_{c2}(0)]/H_{c2}(0);H>H_{c2}(0)]$.

Finally, based on our results, we propose a qualitative picture for QPT, which drastically differs from the Ginzburg-Landau (GL) one, valid close to $T_{c0}$. The latter can be described in terms of a set of long-wavelength fluctuation modes [with $\lambda\gtrsim\xi_{\mathrm{GL}}(T)\gg\xi_{\mathrm{BCS}}$] of the order parameter, with characteristic lifetime $\tau_{\mathrm{GL}}=\pi\hbar/8k_B(T-T_{c0})$. Near the QPT, the order parameter oscillates on much smaller scales—the fluctuation modes with wavelengths up $\xi_{\mathrm{BCS}}$ are excited. Due to the magnetic field, one can imagine that FCPs in this region rotate with the Larmor radius $\sim\xi_{\mathrm{BCS}}$ and cyclotron

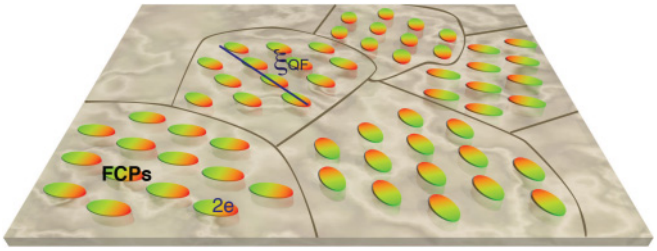


FIG. 4. (Color online) Illustration of the cluster structure of a FCP (2e) liquid above the upper critical field. This picture represents a snapshot at a certain time and would stay that way for time $\tau_{QF}$. The typical size of a coherent FCP cluster is $\xi_{QF}$.

frequency $\omega_c \sim \Delta_{\rm BCS}^{-1}$. We show that close to $H_{c2}(0)$ these FCPs form some kind of quantum liquid with long coherence length $\xi_{\rm QF} \sim \xi_{\rm BCS}/\widetilde{h}^{1/2}$ and slow relaxation $\tau_{\rm QF} \sim \hbar\Delta_{\rm BCS}^{-1}/\widetilde{h}$ (see Fig. 4).

In the following sections and in the appendixes, we show the details of our derivations and calculation and present the general expression for the fluctuation magnetoconductivity of disordered 2D SCs throughout the whole phase diagram. For the calculation of the complete and various fluctuation corrections (by numerical integration and summation), we developed an optimized program which is available at Ref. 18. It can be used as the theoretical basis for the fluctuation spectroscopy of SCs (in the following we use the term "fluctuoscopy"): the study of their behavior in ultrahigh magnetic fields and precise extraction for their physical parameters, like the critical temperature and magnetic field, and the temperature dependence of the phase-breaking time and/or, for example, for the separation of the quantum corrections in studies of the "SC-insulator" transition.

## II. MODEL

We consider a disordered 2D SC characterized by the diffusion coefficient $\mathcal{D}$ placed in a perpendicular magnetic field $H$ at temperatures $T > T_c(H)$. Temperatures should not be too close to the critical temperature and remain beyond the region of critical fluctuations; that is, $T/T_c(H) - 1 \gg \sqrt{{\rm Gi}_{(2)}(H)}$. The Ginzburg-Levanyuk number ${\rm Gi}_{(2)}$ for conductivity (see Ref. 1) in both extremes of the line $H_{c2}(T)$ (at temperatures close to $T_{c0}$ and at zero temperature) is on the order of $(p_F^2 ld)^{-1}$, where $d$ is the SC film thickness, and it can reach values of up to $10^{-2}$. We assume the temperature $T \ll \min\{\tau^{-1},\omega_D\}$ in order to remain in the diffusive regime of electron scattering and in the frameworks of the BCS model ($\tau$ is the electron elastic scattering time on impurities, $\omega_{\rm D}$ is the Debye frequency). The restrictions on magnetic field are dictated by the requirements to be below the regime of Shubnikov-de Haas oscillations [$\omega_c\tau \lesssim 1 \Longleftrightarrow H \lesssim (T_{c0}\tau)^{-1}H_{c2}(0)$, where $\omega_c = 4\mathcal{D}eH$ is the fluctuation Cooper pair cyclotron frequency] and to be below the Clogston limit: $H \lesssim (\varepsilon_F\tau)H_{c2}(0)$, that is, $H/H_{c2}(0) \ll \min\{(T_{c0}\tau)^{-1},\varepsilon_F\tau\}$.

Under these rather nonrestrictive assumptions the dc fluctuation conductivity

$$\delta\sigma^{(\rm fl)}(T,H) = -\lim_{\omega\to 0}\frac{{\rm Im}Q^{(\rm fl)}(\omega,T,H)}{\omega} \tag{1}$$

is determined by the imaginary part of the fluctuation contribution $Q^{(\rm fl)}(\omega,T,H)$ to the electromagnetic response operator.[1] The latter is described graphically by the ten standard diagrams shown inFig. 1. The solid lines denote the one-electron Green's function

$$G(x,x',p_y,p_z,\varepsilon_l) = \sum_k \frac{\varphi_k\left(x - l_H^2 p_y\right)\varphi_k^*\left(x' - l_H^2 p_y\right)}{i\widetilde{\varepsilon}_l - \xi\left(k,p_z\right)},$$

wavy lines correspond to the fluctuation propagator

$$L_n^{-1}(\Omega_k) = -\nu_0\left[\ln\frac{T}{T_{c0}} + \psi\left(\frac{1}{2} + \frac{|\Omega_k| + \omega_c(n+\frac{1}{2})}{4\pi T}\right) - \psi\left(\frac{1}{2}\right)\right], \tag{2}$$

and shaded three- and four-leg blocks indicate the results of the average over elastic impurity scattering of electrons (Cooperons):

$$\lambda_n(\varepsilon_1,\varepsilon_2) = \frac{\tau^{-1}\theta(-\varepsilon_1\varepsilon_2)}{|\varepsilon_1 - \varepsilon_2| + \omega_c(n+1/2) + \tau_\varphi^{-1}}, \tag{3}$$

$$C_n(\varepsilon_1,\varepsilon_2) = \frac{1}{2\pi\nu_0\tau}\frac{\tau^{-1}\theta(-\varepsilon_1\varepsilon_2)}{|\varepsilon_1 - \varepsilon_2| + \omega_c(n+1/2) + \tau_\varphi^{-1}}. \tag{4}$$

Here $\nu_0$ is the one-electron DOS, $n, m$ are the quantum numbers of the Cooper pair Landau states, and $\Omega_k = 2\pi kT$ and $\varepsilon_l = 2\pi T\,(l + 1/2)$ are the bosonic and fermionic Matsubara frequencies, respectively. An important characteristic of these expressions is that they are valid even far from the critical temperature [for temperatures $T \ll \min\{\tau^{-1},\omega_D\}$] and for $|\Omega_k| \ll \omega_D$ and $n \ll (T_{c0}\tau)^{-1}$.

In the appendixes we present the details of the calculation of all ten diagrams performed under the above general assumptions. In the following sections of the main text, we restrict ourselves to the discussion and analysis of the main result: the complete expression of the fluctuations corrections and the individual contributions from AL, MT, DOS, and DCR processes.

## III. RESULTS

The complete expression for the total fluctuation correction to conductivity $\delta\sigma_{xx}^{(\rm tot)}(T,H)$ of a disordered 2D SC in a perpendicular magnetic field that holds in the complete $T$-$H$ phase diagram above the line $H_{c2}(T)$ is given by the sum of

Eqs. (A15), (B7), (C7), and (D10):

$$\delta\sigma_{xx}^{(\mathrm{tot})}(t,h) = \underbrace{\frac{e^2}{\pi}\sum_{m=0}^{\infty}(m+1)\int_{-\infty}^{\infty}\frac{dx}{\sinh^2\pi x}\left\{\frac{[\mathrm{Re}^2(\mathcal{E}_m-\mathcal{E}_{m+1})-\mathrm{Im}^2(\mathcal{E}_m-\mathcal{E}_{m+1})]\,\mathrm{Im}\,\mathcal{E}_m\,\mathrm{Im}\,\mathcal{E}_{m+1}}{|\mathcal{E}_m|^2|\mathcal{E}_{m+1}|^2} - \frac{\mathrm{Re}(\mathcal{E}_m-\mathcal{E}_{m+1})\,\mathrm{Im}(\mathcal{E}_m-\mathcal{E}_{m+1})(\mathrm{Im}\,\mathcal{E}_m\,\mathrm{Re}\,\mathcal{E}_{m+1}+\mathrm{Im}\,\mathcal{E}_{m+1}\,\mathrm{Re}\,\mathcal{E}_m)}{|\mathcal{E}_m|^2|\mathcal{E}_{m+1}|^2}\right\}}_{\delta\sigma_{xx}^{\mathrm{AL}}}$$
$$+\underbrace{\frac{e^2}{\pi}\left(\frac{h}{t}\right)\sum_{m=0}^{M}\frac{1}{\gamma_\phi+\frac{2h}{t}(m+1/2)}\int_{-\infty}^{\infty}\frac{dx}{\sinh^2\pi x}\frac{\mathrm{Im}^2\,\mathcal{E}_m}{|\mathcal{E}_m|^2}}_{\delta\sigma_{xx}^{\mathrm{MT(an)}}+\delta\sigma_{xx}^{\mathrm{MT(reg2)}}} + \underbrace{\frac{e^2}{\pi^4}\left(\frac{h}{t}\right)\sum_{m=0}^{M}\sum_{k=-\infty}^{\infty}\frac{4\mathcal{E}_m''(t,h,|k|)}{\mathcal{E}_m(t,h,|k|)}}_{\delta\sigma_{xx}^{\mathrm{MT(reg1)}}}$$
$$+\underbrace{\frac{4e^2}{\pi^3}\left(\frac{h}{t}\right)\sum_{m=0}^{M}\int_{-\infty}^{\infty}\frac{dx}{\sinh^2\pi x}\frac{\mathrm{Im}\,\mathcal{E}_m\,\mathrm{Im}\,\mathcal{E}_m'}{|\mathcal{E}_m|^2}}_{\delta\sigma_{xx}^{\mathrm{DOS}}} + \underbrace{\frac{4e^2}{3\pi^6}\left(\frac{h}{t}\right)^2\sum_{m=0}^{M}\left(m+\frac{1}{2}\right)\sum_{k=-\infty}^{\infty}\frac{8\mathcal{E}_m'''(t,h,|k|)}{\mathcal{E}_m(t,h,|k|)}}_{\delta\sigma_{xx}^{7-10}}. \tag{5}$$

Here $t = T/T_{c0}$,

$$h = \frac{\pi^2}{8\gamma_E}\frac{H}{H_{c2}(0)} = 0.69\frac{H}{H_{c2}\,(0)},$$

$\gamma_E = e^{\gamma_e}$ ($\gamma_e$ is the Euler constant), $M = (tT_{c0}\tau)^{-1}$, $\gamma_\phi = \pi/(8T_{c0}\tau_\phi)$, $\tau_\phi$ is the phase-breaking time,

$$\mathcal{E}_m \equiv \mathcal{E}_m(t,h,ix) = \ln t + \psi\left[\frac{1+ix}{2}+\frac{2h}{t}\frac{(2m+1)}{\pi^2}\right]-\psi\left(\frac{1}{2}\right),$$

and its derivatives $\mathcal{E}_m^{(p)}(t,h,z) \equiv \partial_z^p\mathcal{E}_m(t,h,z)$. Apart from the detailed derivation of the result [Eq. (5)], one can also do a careful study of the asymptotic expressions for different fluctuation contributions throughout the $h$-$t$ phase diagram, presented in the appendixes. All of them, side by side with the asymptotic expressions for $\delta\sigma_{xx}^{(\mathrm{tot})}$ are summarized in Table I (see also Table II and Fig. 5).

We start the discussion of Table I for domains I–III, corresponding to the GL region of fluctuations close to $T_{c0}$ and in zero magnetic field (domain I). One can see that our general expression Eq. (5) naturally reproduces the well-known AL, MT, and DOS contributions. The only new result here is the explicitly written contribution $\delta\sigma^{(7-10)}$ (diagrams 7–10), which was usually ignored in view of the lack of its divergence close to $T_{c0}$. Nevertheless, one can see that its constant contribution $\sim \ln\ln(T_{c0}\tau)^{-1}$ is necessary for matching the GL results with the neighboring domains VIII and IX. Domains II and III are still described by the GL theory in weak magnetic fields and Eq. (5) reproduces all available asymptotic expressions found in literature.

The most surprising result in Table I is domain IV, the region of QFs (see Fig. 3): One sees that the positive AL (the anomalous MT contribution is equal to the AL one in that domain) decays with decreasing temperature as $T^2$. Moreover, it is exactly canceled by the negative contribution of the four

TABLE I. Asymptotic expressions in different domains, shown in Fig. 5. The first column gives the domain according to that figure and is determined by the $t$ and $h$ regions given in Table II.

| | $\delta\sigma_{xx}^{\mathrm{AL}}$ | $\delta\sigma_{xx}^{\mathrm{MT}}$ | $\delta\sigma_{xx}^{\mathrm{DOS}}$ | $\delta\sigma_{xx}^{7-10}$ | $\delta\sigma_{xx}^{(\mathrm{tot})}$ |
|---|---|---|---|---|---|
| I | $\frac{e^2}{16\epsilon}$ $-\frac{7\zeta(3)e^2}{8\pi^4}\ln\frac{1}{\epsilon}$ | $\frac{e^2}{8(\epsilon-\gamma_\phi)}\ln\frac{\epsilon}{\gamma_\phi}-\frac{14\zeta(3)e^2}{\pi^4}\ln\frac{1}{\epsilon}$ | $-\frac{14\zeta(3)e^2}{\pi^4}\ln\frac{1}{\epsilon}$ | $\frac{e^2}{3\pi^2}\ln\ln\frac{1}{T_{c0}\tau}$ $+O(\epsilon)$ | $\frac{e^2}{16\epsilon}+\frac{e^2}{8(\epsilon-\gamma_\phi)}\ln\frac{\epsilon}{\gamma_\phi}$ $+\frac{e^2}{3\pi^2}\ln\ln\frac{1}{T_{c0}\tau}$ |
| I–III | $\frac{e^2}{2\epsilon}\left(\frac{\epsilon}{2h}\right)^2\left[\psi\left(\frac{1}{2}+\frac{\epsilon}{2h}\right)-\psi\left(\frac{1}{2}\right)-\frac{h}{\epsilon}\right]$ | $\frac{e^2}{8}\frac{1}{\epsilon-\gamma_\phi}\left[\psi\left(\frac{1}{2}+\frac{t\epsilon}{2h}\right)-\psi\left(\frac{1}{2}+\frac{t\gamma_\phi}{2h}\right)\right]$ $-\frac{14\zeta(3)e^2}{\pi^4}\left[\ln\left(\frac{t}{2h}\right)-\psi\left(\frac{1}{2}+\frac{t\epsilon}{2h}\right)\right]$ | $-\frac{14\zeta(3)e^2}{\pi^4}\left[\ln\left(\frac{t}{2h}\right)-\psi\left(\frac{1}{2}+\frac{t\epsilon}{2h}\right)\right]$ | $\frac{e^2}{3\pi^2}\ln\ln\frac{1}{T_{c0}\tau}$ $+O(\max[\epsilon,h^2])$ | |
| IV | $\frac{4e^2\gamma_E^2t^2}{3\pi^2h^2}$ | $-\frac{2e^2}{\pi^2}\ln\frac{1}{h}-\frac{2\gamma_Ee^2}{\pi^2}\left(\frac{t}{h}\right)$ | $-\frac{4e^2\gamma_E^2t^2}{3\pi^2h^2}$ | $\frac{4e^2}{3\pi^2}\ln\frac{1}{h}+\frac{4\gamma_Ee^2}{3\pi^2}\frac{t}{h(t)}$ | $-\frac{2e^2}{3\pi^2}\left(\ln\frac{1}{h}+\frac{\gamma_Et}{h}\right)$ |
| V | $\frac{2\gamma_Ee^2}{\pi^2}\left(\frac{t}{h}\right)$ | $-\frac{2e^2}{3\pi^2}\ln\frac{1}{4\gamma_Et}$ | $-\frac{2\gamma_Ee^2}{\pi^2}\left(\frac{t}{h}\right)$ | $\frac{4\gamma_Ee^2}{3\pi^2}\frac{t}{h}$ | $\frac{4\gamma_Ee^2}{3\pi^2}\frac{t}{h}$ |
| VI–VII | $\frac{e^2}{4}\frac{t}{h-h_{c2}(t)}$ | $-\frac{2e^2}{\pi^2}\ln\frac{2h}{\pi^2t}$ | $-\frac{e^2}{4}\frac{t}{h-h_{c2}(t)}$ | $\frac{e^2}{6}\frac{t}{h-h_{c2}(t)}$ | $\frac{e^2}{6}\frac{t}{h-h_{c2}(t)}$ |
| VIII | $\frac{e^2}{6\pi^2}\frac{C_1}{\ln^3t}$ | $-\frac{e^2}{\pi^2}\ln\frac{\ln\frac{1}{T_{c0}\tau}}{\ln t}+\frac{\pi^2e^2}{192}\frac{\ln\frac{\pi^2}{2\gamma_\phi}}{\ln^2t}$ | $-\frac{\pi^2e^2}{192}\frac{1}{\ln^2t}$ | $\frac{e^2}{3\pi^2}\ln\frac{\ln\frac{1}{T_{c0}\tau}}{\ln t}$ | $-\frac{2e^2}{3\pi^2}\ln\frac{\ln\frac{1}{T_{c0}\tau}}{\ln t}$ |
| IX | $\frac{\pi^2e^2}{192}\left(\frac{t}{h}\right)^2\frac{C_2}{\ln^3\frac{2h}{\pi^2}}$ | $-\frac{e^2}{\pi^2}\ln\frac{\ln\frac{1}{T_{c0}\tau}}{\ln\frac{2h}{\pi^2}}+\frac{7\zeta(3)\pi^2e^2}{768}\left(\frac{t}{h}\right)^2\frac{1}{\ln^2\frac{2h}{\pi^2}}$ | $-\frac{7\zeta(3)\pi^2e^2}{384}\left(\frac{t}{h}\right)^2\frac{1}{\ln^2\frac{2h}{\pi^2}}$ | $\frac{e^2}{3\pi^2}\ln\frac{\ln\frac{1}{T_{c0}\tau}}{\ln\frac{2h}{\pi^2}}$ | $-\frac{2e^2}{3\pi^2}\ln\frac{\ln\frac{1}{T_{c0}\tau}}{\ln\frac{2h}{\pi^2}}$ $-\frac{7\zeta(3)\pi^2e^2}{768}\left(\frac{t}{h}\right)^2\frac{1}{\ln^2\frac{2h}{\pi^2}}$ |

TABLE II. Explanation of the different domains with $t$ and $h$ ranges. Here $\epsilon = \ln t$.

| Domain | $t$ and $h$ range | Description |
|---|---|---|
| I | $h = 0, \epsilon \ll 1$ | Zero field, near $T_{c0}$ |
| II | $h - h_{c2} \sim \epsilon \ll 1$ | Near $T_{c0}$-reflected $h_{c2}$ line |
| III | $h - h_{c2}(t) \ll 1, \epsilon \ll 1$ | Near $h_{c2}$ line |
| I–III | $h \ll 1, \epsilon \ll 1$ | GL region |
| IV | $t \ll h - h_{c2}(t)$ | Region of quantum fluctuations |
| V | $\widetilde{h} \sim t \ll 1$ | Quantum to classical |
| VI | $\widetilde{h} \lesssim t \ll 1$ | Classical, near $h_{c2}(t \ll 1)$ |
| VII | $h - h_{c2}(t) \lesssim t \ll h_{c2}(t)$ | Classical, strong fields |
| VIII | $\ln t \gtrsim 1, h \ll t$ | High temperatures |
| IX | $h \gg \max\{1,t\}$ | High magnetic fields |

DOS-like diagrams 3–6:

$$\delta\sigma_{xx}^{\mathrm{AL}} = \delta\sigma_{xx}^{\mathrm{MT(an)}} = -\delta\sigma_{xx}^{\mathrm{DOS}} = \frac{4e^2\gamma_E^2 t^2}{3\pi^2\widetilde{h}^2}. \tag{6}$$

The total fluctuation contribution to conductivity $\delta\sigma_{xx}^{(\mathrm{tot})}$ in this important region ($t \ll \widetilde{h}$) is *completely determined by the renormalization of the diffusion coefficient* (the regular part of the MT contribution and diagrams 7–10). It turns out to be negative and at zero temperature diverges logarithmically when the magnetic field approaches $H_{c2}(0)$. The nontrivial fact following from Eq. (5) is that an increase of temperature at a fixed value of the magnetic field in this domain mainly results in a further decrease of conductivity,

$$\delta\sigma_{xx}^{(\mathrm{tot})} = -\frac{2e^2}{3\pi^2}\ln\frac{1}{\widetilde{h}} - \frac{2\gamma_E e^2}{3\pi^2}\frac{t}{\widetilde{h}} + O\left[\left(\frac{t}{\widetilde{h}}\right)^2\right], \tag{7}$$

and only at the boundary with domain V, when $t \sim \widetilde{h}$, does the total fluctuation contribution $\delta\sigma_{xx}^{(\mathrm{tot})}$ pass through a minimum and start to grow. Such nonmonotonic behavior of the conductivity close to $H_{c2}(0)$ was observed multiple times in experiments.[19,20] In Ref. 21 a detailed analysis of fluctuation corrections was performed using the low temperature asymptotics of Ref. 15.

Domain V describes the transition regime between quantum and classical fluctuations, while in domains VI–VII, extended along the line $H_{c2}(T)$, SFs have already classical (but non-GL) character. In all these three regions one observes exactly the same cancellation of the AL and DOS contributions as in domain IV and $\delta\sigma_{xx}^{(\mathrm{tot})}$ is determined by the negative DCR contribution.

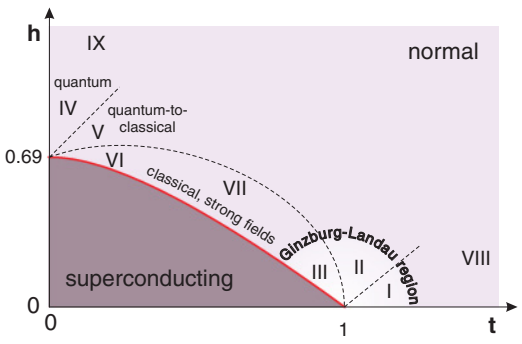


FIG. 5. (Color online) Schematic representation of the regions of different behavior of fluctuation conductivity in the $h$-$t$ diagram. See Table II for more explanations on the domains.

Finally, in the peripheral domains VIII–IX, the direct positive contribution of fluctuation Cooper pairs (AL) to conductivity decays faster than all the other: $\sim\ln^{-3}(T/T_{c0})$. We stress, that this exact result differs from the evaluation of the AL paraconductivity far from the transition of Ref. 7, but is in complete agreement with the high temperature asymptotic expression for the paraconductivity of a clean 2D SC (see Ref. 22). This agreement seems natural: Fluctuation Cooper pair transport is insensitive to impurity scattering. The anomalous MT contribution, in complete accordance with Refs. 7 and 8, decays as $\sim\ln\gamma_\phi^{-1}/\ln^{-2}(T/T_{c0})$. The contribution of diagrams 3–6 also decays as $\ln^{-2}(T/T_{c0})$, but without the large factor $\ln\gamma_\phi^{-1}$. Finally, the regular MT contribution together with the ones from diagrams 7–10 decay extremely slow, in fact, double logarithmically:

$$\delta\sigma_{xx}^{\mathrm{DCR}} = -\frac{2e^2}{3\pi^2}\left(\ln\ln\frac{1}{T_{c0}\tau} - \ln\ln\frac{T}{T_{c0}}\right). \tag{8}$$

Up to the numerical prefactor this expression coincides with the results of Refs. 7 and 9.

Equation (5) provides the basis for a "fluctuoscope" for SCs, that is, the extraction of its microscopic parameters from the analysis of fluctuation corrections. Indeed, one can see that $\delta\sigma_{xx}^{(\mathrm{tot})}$ depends on two superconducting parameters: $T_{c0}, H_{c2}(0)$, the elastic scattering time $\tau$, and (temperature-dependent) phase-breaking time $\tau_\phi(T)$. The elastic scattering time can be obtained from the normal state properties of the SC, while the Eq. (5) can become the instrument for the precise determination of the critical temperature $T_{c0}$ (instead of the often-used rule "half width of transition") and $H_{c2}(0)$. Moreover, it can be an invaluable tool for the study of the temperature dependence of the phase-breaking time $\tau_\phi(T)$.

The exemplary surface of $\delta\sigma_{xx}^{(\mathrm{tot})}(T,H)$ presented in Fig. 2 for $T_{c0}\tau = 10^{-2}$ and $T_{c0}\tau_\phi = 10$ shows that the value of $\tau_\phi$ determines the behavior of fluctuation corrections only in the region of low fields. It is convenient to analyze Fig. 2 side by side with Fig. 3 where lines $\delta\sigma_{xx}^{(\mathrm{tot})}(T,H) = \mathrm{const}$ through the phase diagram are shown. It is interesting to note that the numerical analysis of Eq. (5) shows that the logarithmic asymptotic Eq. (7) is valid only within an extremely narrow field range $\widetilde{h} \lesssim 10^{-6}$.

In order to get a broader overview of the richness of our main result, we compiled several magnetoconductivity single-parameter dependencies (cuts through the "surface" at constant $t$ or $h$) in Fig. 6. Each individual panel (a) through (j) of this figure shows the total FC for six different values of $T_{c0}\tau_\phi$ between 0.1 and 50 and fixed $T_{c0}\tau = 10^{-3}$. If $\delta\sigma = 0$ is within plot range, it is marked by a horizontal dashed line, and the critical magnetic fields $H_{c2}(T)$ are shown as (red) vertical dashed lines. Panels (a) to (e) show $\delta\sigma(t)$ for different magnetic fields below ($h = 0.01, 0.35$, superconducting region marked by "*SC*"), at ($h = 0.69$), and above ($h = 0.75, 1.0$) the zero-temperature critical field $H_{c2}(0)$. The legend key of panel (a) applies to all panels. The behavior is as expected from the above discussion, but it is very educative to take a closer look at the behavior near the QPT [panel (c)]: As mentioned above, the asymptotic expression for the quantum regime is

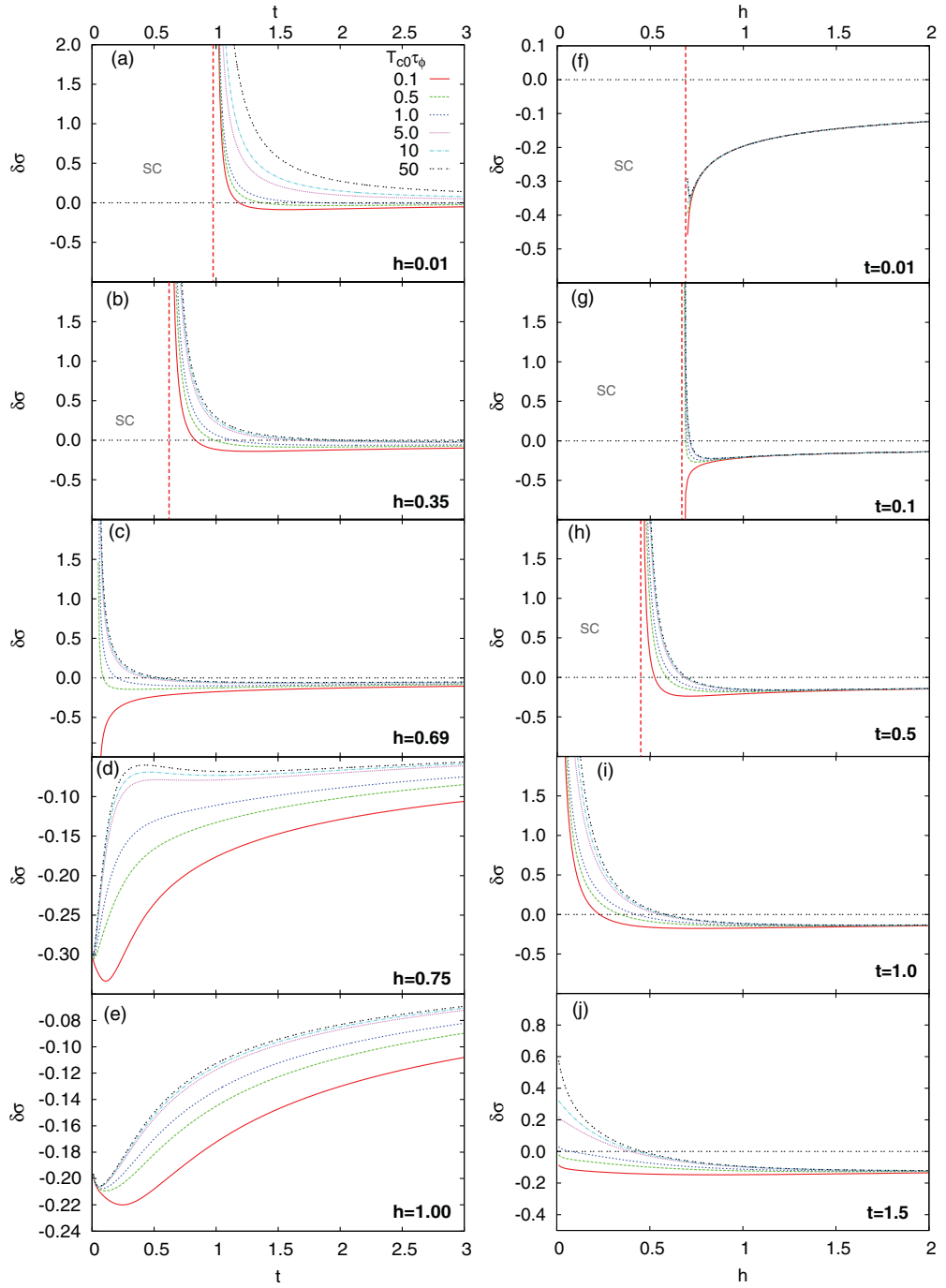


FIG. 6. (Color online) Total fluctuation conductivity for different $T_{c0}\tau_\phi$ for several constant temperatures $t$ and magnetic fields $h$. (a)–(e) $\delta\sigma(t)$ for different magnetic fields below ($h = 0.01,0.35$, superconducting region marked by "*SC* "), at ($h = 0.69$), and above ($h = 0.75,1.0$) the zero-temperature critical field $H_{c2}(0)$. The legend key of panel (a) applies to all panels. Note that the value of $T_{c0}\tau_\phi$ near the transition at $t = 0$ can determine the sign of the fluctuation conductivity; however, at very low temperatures the FC becomes independent of the phase-breaking time and all lines coalesce, which is not resolved in that plot. (f)–(j) $\delta\sigma(h)$ for constant temperatures, below ($t = 0.01,0.1,0.5$), at ($t = 1.0$), and above ($t = 1.5$) the transition temperature $T_{c0}$. All plots are calculated for $T_{c0}\tau = 10^{-3}$. If $\delta\sigma = 0$ is within plot range, it is marked by a horizontal dashed line, and the critical magnetic fields $H_{c2}(T)$ are shown as (red) vertical dashed lines. See detailed discussion in the text.

only valid at extremely small temperatures, which cannot be resolved in this plot. Therefore, one sees in particular for the smallest $T_{c0}\tau_\phi$ value a sharp dip in the FC at low temperatures, which will eventually coalesce with all other curves at even lower temperature (not visible) and become independent of the phase-breaking time, as can be seen at larger $h$ in panels (d) and (e).

Panels (f) to (j) show $\delta\sigma(h)$ for constant temperatures, below ($t = 0.01,0.1,0.5$), at ($t = 1.0$), and above ($t = 1.5$) the transition temperature $T_{c0}$. Here again it is seen in panel (f)

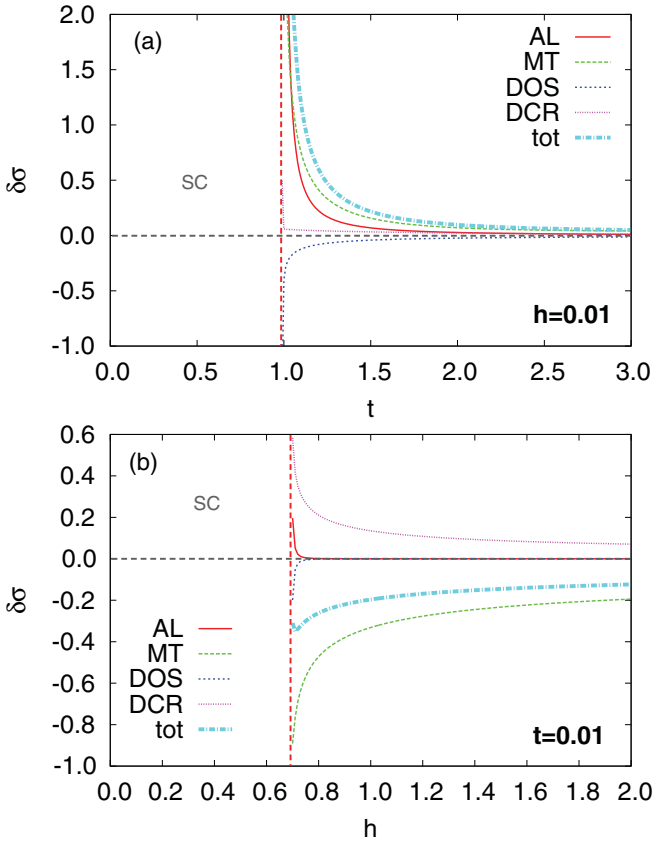


FIG. 7. (Color online) Fluctuation conductivity contributions: AL, MT, DOS, DCR, and total (tot) for $T_{c0}\tau = 10^{-3}$ and $T_{c0}\tau_\phi = 5$. (a) Temperature dependence at low field $h = 0.01$; (b) field dependence at low temperature $t = 0.01$.

that in the quantum regime the FC is mostly independent of the phase-breaking time and only close to the QPT a separation of the curves becomes visible since even the small temperature $t = 0.01$ becomes of order $\tilde{h}$ or even larger and the asymptotic expression does not hold anymore.

In Fig. 7 we plotted two particular curves of Fig. 6 in more detail, showing the different contributions from the diagram groups (a)–(d) of Fig. 1. These are the curves for $T_{c0}\tau_\phi = 5$ at lowest magnetic field $h = 0.01$ [in panel (a)] and temperature $t = 0.01$ [in panel (b)]. Comparing these curves to the asymptotics of Table I, one sees that the behavior near $T_{c0}$ is as expected [see panel (a)], and in particular the contribution from diagrams 7–10 is negligible. However, in the quantum regime it becomes the dominating contribution, rendering the total FC negative and only close to the QPT is it canceled by the MT contribution.

Despite Eq. (5) being a closed expression, its specific evaluation in the most general case requires sophisticated numerical summation and integration. While being straight-forward, one might encounter technical difficulties in the evaluation of the complex polygamma functions $\psi^{(n)}(z)$. Moreover, the summation cutoff parameter $M$ can reach extremely large values at low temperatures [experimental values $(T_{c0}\tau)^{-1}_{\rm exp}$ for materials near the SC-insulator transition can be on the order $10^6$], which slows down the numerical procedure significantly. The latter difficulty can be partially overcome by evaluation of

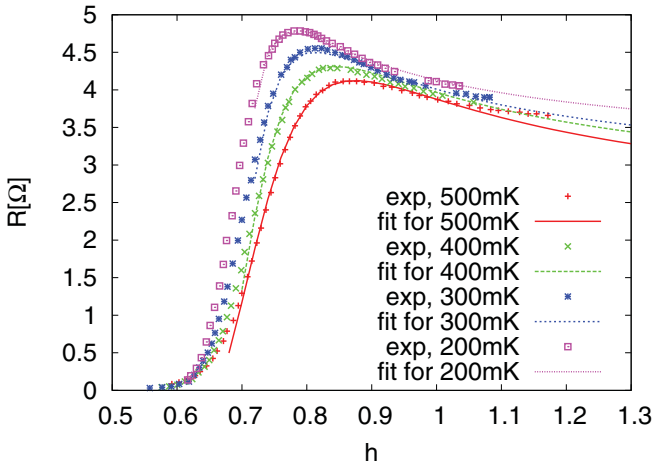


FIG. 8. (Color online) Comparison to resistivity measurements in thin indium oxide films, published in Ref. 23. Here we present the data taken from Fig. 4(a) of Ref. 23 for the "Weak" sample with thickness 30 nm, $T_{c0} = 3.35$ K, and $B_{c2}(0) = 13$ T. We fitted the resistivity $R$ for temperatures 0.2, 0.3, 0.4, and 0.5 K using our full expression for $\delta\sigma$ with the experimentally found $T_{c0}$. For $B_{c2}(0)$ we fitted a slightly larger value of 13.7 T and $T_{c0}\tau_\phi = 5 \pm 1$.

the slowly divergent tails of the $m$ sums in Eq. (5) as integrals. Here we should also note that for fitting purposes one does not need to choose the real, often extremely small, experimental values $(T_{c0}\tau)_{\rm exp}$. To save CPU time, one can assume the value $(T_{c0}\tau)_{\rm num}$ of this parameter to be much larger than $(T_{c0}\tau)_{\rm exp}$ (but still much less than $T_{c0}\tau_\phi$) and only at the very end to shift the final expression by $\ln\ln\frac{(T_{c0}\tau)_{\rm num}}{(T_{c0}\tau)_{\rm exp}}$. Nevertheless, the numerics of the problem remains challenging: For the surface plot in Fig. 2 we evaluated $10^6$ values for $\delta\sigma$ with the modest assumption $(T_{c0}\tau)_{\rm num} = 0.01$, yet it still took 3 months of single CPU time for its calculation. Our optimized tool for the evaluation of Eq. (5) can be found in 18.

## IV. COMPARISON WITH EXPERIMENTAL RESULTS

A main aspect of this work is that the complete expression [Eq. (5)] can be used to extract experimental parameters of thin superconducting films from measured data (fluctuoscopy). In particular, the critical temperature $T_{c0}$, the critical magnetic field $H_{c2}(0)$, and the phase-breaking time $\tau_\phi$.

As an example of the practical use for our results, we fitted a set of experimental data by comparing our general Eq. (5) to resistivity measurements in thin disordered indium oxide films, presented in Ref. 23. Figure 8 shows the low-temperature data for one sample (referred to as "Weak" in Ref. 23) of a film with thickness 30 nm, transition temperature $T_{c0} = 3.35$ K, and critical magnetic field $B_{c2}(0) = 13$ T. The resistivity was measured, depending on magnetic field, for low temperature values $T = 200, 300, 400, 500$ mK. We plotted the theoretical expression for $\delta\sigma_{xx}^{(\rm tot)}$ using the fitting parameter values $B_{c2}(0) = 13.7$ T, $T_{c0}\tau_\phi = 5 \pm 1$, and the experimentally found value of $T_{c0} = 3.35$ K. Overall, the fitted FC curves show good agreement with the results of the measurements.

At this point it is important to remark, that $\tau_\phi$ depends on temperature in general, such that for a better fit one needs first to analyze FC data at constant temperatures to extract $\tau_\phi(T)$

and then fit temperature-dependent data. This way one can obtain precise values for the otherwise-difficult-to-determine experimental parameters $T_{c0}$, $H_{c2}(0)$, and $\tau_\phi(T)$.

## V. QUANTUM LIQUID OF FCP IN THE VICINITY OF $H_{c2}(0)$

An analysis of the obtained results allows us to offer a qualitative picture of the QPT occurring in the vicinity of $H_{c2}(0)$ at very low temperatures. Above we presented the complete microscopic calculation. However, it is instructive to start our discussion of the QFs by describing and refreshing the qualitative picture of SFs in the vicinity of $T_{c0}$, in the GL region,[1] for further comparison. In domains I–III, the lifetime of fluctuation-induced Cooper pairs $\tau_{GL}$ can be obtained in the simplest way by using the uncertainty principle. Indeed, $\tau_{GL} \sim \hbar/\Delta E$, where $\Delta E$ is the energy difference $k_B(T - T_{c0})$ ensuring that $\tau_{GL}$ should become infinite at the transition point. This yields the standard GL time

$$\tau_{GL} \sim \hbar/k_B(T - T_{c0}) \sim \hbar/(k_B T_{c0}\epsilon), \tag{9}$$

where $\epsilon = (T - T_{c0})/T_{c0} \ll 1$ is the reduced temperature. In its turn the coherence length $\xi_{GL}(T)$ can be estimated as the distance which two electrons move apart during the GL time:

$$\xi_{GL}(\epsilon) = (\mathcal{D}\tau_{GL})^{1/2} \sim \xi_{BCS}/\sqrt{\epsilon}.$$

Here $\xi_{BCS} \sim \sqrt{\mathcal{D}/T_{c0}}$ is the BCS coherence length and $\mathcal{D}$ is the diffusion coefficient. The fluctuating order parameter $\Delta^{(fl)}(\mathbf{r},t)$ varies close to $T_{c0}$ on a larger scale $\xi_{GL}(\epsilon) \gg \xi_{BCS}$. The ratio of the FCP concentration to the corresponding effective mass with logarithmic accuracy can be estimated as $n_{c.p.}/m_{c.p.} \sim \xi_{GL}^{2-D}(\epsilon)$ and in the 2D case assumed as constant (which is the case we will discuss in the following).[1]

The two principal fluctuation contributions to conductivity close to $T_{c0}$ are positive and originate from a direct FCP charge transfer (AL contribution)

$$\delta\sigma_{xx}^{AL} \sim (n_{c.p.}/m_{c.p.})e^2\tau_{GL} \sim e^2/\hbar\epsilon \tag{10}$$

and from the specific quantum process of one-electron charge transfer related to coherent scattering of electrons on elastic impurities, which leads to the formation of FCPs (anomalous MT contribution),

$$\delta\sigma_{xx}^{MT(an)} \sim \frac{e^2}{\hbar\epsilon}\ln(\epsilon/\gamma_\phi).$$

However, these two contributions do not capture the complete effect of fluctuations on conductivity. The involvement of quasiparticles in the fluctuation pairing results in their absence at the Fermi level, that is, in the opening of a pseudogap in the one-electron spectrum, and consequently decreases the one-particle Drude-like conductivity. Such an indirect effect of the FCP formation is usually referred to as the DOS contribution. Being proportional to the concentration of the FCPs $n_{c.p.}$, the DOS contribution formally appears by integration of the Fourier-component $\langle|\Delta^{(fl)}(\mathbf{q},\omega)|^2\rangle$ of the order parameter over all long-wavelength fluctuation modes ($q \lesssim \xi_{BCS}^{-1}\sqrt{\epsilon}$), in the static approximation ($\omega \to 0$) given by

$$\delta\sigma_{xx}^{DOS} \sim -\frac{2n_{c.p.}e^2\tau}{m_e} \sim -e^2\int\frac{\xi_{BCS}^2 d^2\mathbf{q}}{\epsilon + \xi_{BCS}^2 q^2} \sim -\frac{e^2}{\hbar}\ln\frac{1}{\epsilon}. \tag{11}$$

One sees that the DOS contribution has the opposite sign with respect to the AL and MT contributions, but close to $T_{c0}$ does not compete with those, since it turns out to be less singular as a function of temperature.

Finally, the one-electron diffusion coefficient is renormalized in the presence of fluctuation pairing (DCR). Close to $T_{c0}$ this contribution is not singular in $\epsilon$ (see Table I) and was usually ignored in the literature, but as was mentioned before, it becomes of primary importance relatively far from $T_{c0}$, and at very low temperatures. It is due to $\delta\sigma_{xx}^{DCR}$ that the sign of the total contribution of fluctuations to conductivity $\delta\sigma_{xx}^{(tot)}$ changes in a wide domain of the phase diagram and in particular close to $T = 0$, in the region of QFs (see Fig. 3, where the regions with dominating fluctuation contributions to magnetoconductivity are shown).

At zero temperature and fields above $H_{c2}(0)$, the systematics of the fluctuation contributions to the conductivity changes considerably with respect to that close to $T_{c0}$. Due to the collisionless rotation of FCPs (they do not "feel" the presence of elastic impurities; all information concerning electron scattering is already included in the effective mass of the Cooper pairs) they do not contribute directly to the longitudinal (along the applied electric field) electric transport [analogous to the suppression of the one-electron conductivity in strong magnetic fields ($\omega_c\tau \gg 1$): $\delta\sigma_{xx}^{(e)} \sim (\omega_c\tau)^{-2}$, see Ref. 24] and the AL contribution to $\delta\sigma_{xx}^{(tot)}$ becomes zero. The anomalous MT and DOS contributions tend to zero as well but for different reasons. Namely, the former vanishes since magnetic fields as large as $H_{c2}(0)$ completely destroy the phase coherence, whereas the latter disappears since magnetic field suppresses the fluctuation gap in the one-electron spectrum. Therefore, the effect of fluctuations on the conductivity at zero temperature is reduced to the renormalization of the one-electron diffusion coefficient. FCPs in the quantum region occupy the LLL, but all dynamic fluctuations in the frequency interval from 0 to $\Delta_{BCS}$ have to be taken into account. The corresponding fluctuation propagator at zero temperature close to $H_{c2}(0)$ has the form [see Eq. (A22)]

$$L_0(\omega) = -\nu_0^{-1}\frac{1}{\widetilde{h} + \omega/\Delta_{BCS}}$$

and

$$\delta\sigma_{xx}^{DCR} \sim -\frac{e^2}{\Delta_{BCS}}\int_0^{\Delta_{BCS}}\frac{d\omega}{\widetilde{h} + \frac{\omega}{\Delta_{BCS}}} \sim -\frac{e^2}{\hbar}\ln\frac{1}{\widetilde{h}}. \tag{12}$$

The parameter $\widetilde{h} = [H - H_{c2}(0)]/H_{c2}(0)$ plays the same role as the reduced temperature $\epsilon$ in the case of the classical transition; $\Delta_{BCS}$ is the BCS value of the gap at zero temperature in zero field.

While the denominator of the integrand in Eq. (11) defines the characteristic wavelength $\xi_{GL}(T)$ of the fluctuation modes close to $T_{c0}$, the one in Eq. (12) defines the characteristic coherence time $\tau_{QF}(\widetilde{h})$ of QFs near $H_{c2}(0)$ (where $t \ll \widetilde{h}$). The value of the integral is determined by its lower cutoff $\omega_{QF} \sim \Delta_{BCS}\widetilde{h}$, and the corresponding time scale is

$$\tau_{QF} \sim \hbar(\Delta_{BCS}\widetilde{h})^{-1}. \tag{13}$$

One sees that the functional form of $\tau_{QF}$ is completely analogous to that of $\tau_{GL}$: $\Delta_{BCS} \triangleq T_{c0}$ and the reduced field $\widetilde{h}$

plays the role of reduced temperature $\epsilon$. Equation (13) can also be obtained from the uncertainty principle. Indeed, the energy, characterizing the proximity to the QPT is $\Delta E = \hbar\omega_c(H) - \hbar\omega_c[H_{c2}(0)] \sim \Delta_{\rm BCS}\widetilde{h}$ and namely this value should be used in the Heisenberg relation instead of $k_B(T - T_{c0})$, as was done in the vicinity of $T_{c0}$. The spatial coherence scale $\xi_{\rm QF}(\widetilde{h})$ can be estimated from the value of $\tau_{\rm QF}$ analogously to the consideration near $T_{c0}$. Namely, two electrons with coherent phase starting from the same point get separated by the distance

$$\xi_{\rm QF}(\widetilde{h}) \sim (D\tau_{\rm QF})^{1/2} \sim \xi_{\rm BCS}/\sqrt{\widetilde{h}}$$

after time $\tau_{\rm QF}$.

To clarify the physical meaning of $\tau_{\rm QF}$ and $\xi_{\rm QF}$, note that near the QPT at zero temperature, where $H \to H_{c2}(0)$, the fluctuations of the order parameter $\Delta^{(\rm fl)}(\mathbf{r},t)$ become highly inhomogeneous, contrary to the situation near $T_{c0}$. Indeed, below $H_{c2}(0)$, the spatial distribution of the order parameter at finite magnetic field reflects the appearance of Abrikosov vortices with average spacing [close to $H_{c2}(0)$ but in the region where the notion of vortices is still adequate] equal to

$$a\,(H) = \xi_{\rm BCS}/\sqrt{H/H_{c2}\,(0)} \to \xi_{\rm BCS}.$$

Therefore, one expects that close to and above $H_{c2}(0)$ the fluctuation order parameter $\Delta^{(\rm fl)}(\mathbf{r},t)$ also has a "vortexlike" spatial structure and varies over the scale $\xi_{\rm BCS}$ and being preserved over time $\tau_{\rm QF}$. In the language of FCPs, one describes this situation in the following way: A FCP at zero temperature and in magnetic field close to $H_{c2}(0)$ rotates with Larmor radius $r_L \sim v_{\rm F}/\omega_{\rm c}[H_{c2}(0)] \sim v_{\rm F}/\Delta_{\rm BCS} \sim \xi_{\rm BCS}$, which represents its effective size. During time $\tau_{\rm QF}$ two initially selected electrons participate in multiple fluctuating Cooper pairings maintaining their coherence. The coherence length $\xi_{\rm QF}(\widetilde{h}) \gg \xi_{\rm BCS}$ is thus a characteristic size of a cluster of such coherently rotating FCP, and $\tau_{\rm QF}$ estimates the lifetime of such a *flickering* cluster. One can view the whole system as an ensemble of flickering domains of coherently rotating FCP, precursors of vortices (see Fig. 4).

In view of the qualitative picture of SFs in the regime of the QPT, let us continue with the scenario of Abrikosov lattice defragmentation: Approaching $H_{c2}(0)$ from below, puddles of fluctuating vortices are formed, which are nothing more than FCPs rotating in a magnetic field. Their characteristic size is $\xi_{\rm QF}(|\widetilde{h}|)$, and they flicker in the characteristic time $\tau_{\rm QF}(|\widetilde{h}|)$. In this situation, the supercurrent can still flow through the sample until these puddles do not break the last percolating superconductive channel. The corresponding field determines the value of the by QFs renormalized second critical field: $H^*_{c2}(0) = H_{c2}(0)[1 - 2{\rm Gi}\ln(1/{\rm Gi})]$ (see Ref. 1). Above this field no supercurrent can flow through the sample anymore; that is, the system is in the normal state. Nevertheless, as demonstrated by the above estimates, its properties are strongly affected by the QF. Fragments of the Abrikosov lattice can be still observed in this region by the following Gedanken experiment: The clusters of rotating FCPs ("ex-vortices") of size $\xi_{\rm QF}$ with some kind of the superconducting order should be found in the background of the normal state if one takes a picture with exposure time shorter than $\tau_{\rm QF}$. For exposure times longer than $\tau_{\rm QF}$, the picture is smeared out and no traces of the Abrikosov vortex state can be found. However, the detailed nature of the order which exists there is still unclear. It would be attractive to identify these clusters with fragments of the Abrikosov lattice, but most probably this is some kind of quantum FCP liquid. Indeed, the presence of structural disorder can result in the formation of a hexatic phase close to $H^*_{c2}(0)$, where the translational invariance no longer exists, while at the same time conserving the orientational order or the vortices.

## VI. DISCUSSION

In terms of the introduced QF characteristics $\tau_{\rm QF}$ and $\xi_{\rm QF}$, one can understand the meaning of already found microscopic QF contributions to different physical values in the vicinity of $H_{c2}(0)$ and derive others which are related.

### A. In-plane conductivity

For example, the physical meaning of Eq. (6) can be understood as follows: One could estimate the FCP conductivity by merely replacing $\tau_{\rm GL} \to \tau_{\rm QF}$ in the classical AL expression (10), which would give $\delta\widetilde{\sigma}^{AL} \sim e^2\tau_{\rm QF}$. Nevertheless, as we already noticed, a FCP at zero temperature cannot drift along the electric field but only rotates around a fixed center. As temperature deviates from zero, FCPs can change their state due to the interaction with the thermal bath; that is, their hopping to an adjacent rotation trajectory along the applied electric field becomes possible. This means that FCP can participate in longitudinal charge transfer now. This process can be mapped onto the paraconductivity of a granular SC[25] at temperatures above $T_{c0}$, where the FCP tunneling between grains occurs in two steps: First one electron jumps, then the second follows. The probability of each hopping event is proportional to the intergrain tunneling rate $\Gamma$. To conserve the superconducting coherence between both events, the latter should occur during the FCP lifetime $\tau_{\rm GL}$. The probability of FCPs tunneling between two grains is determined by the conditional probability of two one-electron hopping events and is proportional to $W_\Gamma = \Gamma^2\,\tau_{\rm GL}$. Coming back to the situation of FCPs above $H_{c2}(0)$, one can identify the tunneling rate with temperature $T$ while $\tau_{\rm GL}$ corresponds to $\tau_{\rm QF}$. Therefore, in order to obtain a final expression, $\delta\widetilde{\sigma}^{\rm AL}$ should be multiplied by the probability factor $W_{\rm QF} = t^2\tau_{\rm QF}$ of the FCP hopping to the neighboring trajectory:

$$\delta\sigma^{\rm AL}_{xx} \sim \delta\widetilde{\sigma}^{\rm AL}W_{\rm QF} \sim e^2t^2/\widetilde{h}^2,$$

which corresponds to the asymptotic Eq. (6).

### B. Magnetic susceptibility

In order to estimate the contribution of QFs to the fluctuation induced magnetic susceptibility of the SC in the vicinity of $H_{c2}(0)$, one can apply the Langevin formula to a coherent cluster of FCPs and identify its average size by the rotator radius. One finds

$$\chi^{\rm AL} = \frac{e^2n_{\rm c.p.}}{m_{\rm c.p.}c}\langle\xi^2_{\rm QF}(\widetilde{h})\rangle \sim \xi^2_{\rm BCS}/c\widetilde{h}$$

in complete agreement with the result of Ref. 15.

### C. Nernst coefficient

One further reproduces the contribution of QFs to the Nernst coefficient. Close to $H_{c2}(0)$ the chemical potential of FCPs can be identified as $\mu_{\rm FCP} = \hbar\omega_c[H_{c2}(0)] - \hbar\omega_c(H)$ [as in Ref. 13, close to $T_{c0}$, $\mu_{\rm FCP} = k_B(T_{c0} - T)$]. The corresponding derivative is $d\mu_{\rm FCP}/dT \sim dH_{c2}(T)/dT \sim -T/\Delta_{\rm BCS}$. Using the relation between the latter and the Nernst coefficient, it is possible to reproduce one of the results of Ref. 13:

$$\nu^{\rm AL} \sim [\tau_{\rm QF}/m_{\rm c.p.}]d\mu_{\rm FCP}/dT \sim \xi^2_{\rm BCS}t/\widetilde{h}.$$

### D. Transversal magnetoresistance above $H_{c2}(0)$

The proposed qualitative approach can also explain the nonmonotonic behavior of the transversal magnetoresistance observed in the *layered* organic SC $\kappa-$(BEDT$-$TTF)$_2$Cu(NCS)$_2$ above $H_{c2}(0)$ at low temperatures.[26] Indeed, the motion of FCPs along the $z$ axis in such a system has hopping character and the quasiparticle spectrum can be assumed to have the form of a corrugated cylinder. Close to $T_{c0}$ the fluctuation magnetoconductivity tensor in this model was already studied in detail in Ref. 6. There it was demonstrated that the transverse paraconductivity in that case is suppressed by the square of the small anisotropy parameter $(\xi_z/\xi_x)^2$, while the dependence on the reduced temperature $\epsilon$ is even more singular than in plane. In terms of the GL FCP lifetime (9), it can be written as

$$\delta\sigma^{\rm AL}_{zz}(\epsilon) = \frac{4e^2\xi_z^4}{\pi^2\xi^2_{xy}s^3}T^2_{c0}\tau^2_{\rm GL}(\epsilon), \qquad (14)$$

where $s$ is the interlayer distance. In principle, this result could be obtained, even from the Drude formula applied to the FCP charge transfer [see above, how Eq. (10) for $\delta\sigma^{\rm AL}_{xx}(\epsilon)$ was obtained] combined with the above speculations regarding the hopping of FCPs along the $z$ axis.[25] This general approach, which does not involve the GL scheme, allows us to map Eq. (14) in the case of the QPT by just replacing $\tau_{\rm GL}(\epsilon) \to \tau_{\rm QF}(\widetilde{h})$:

$$\delta\sigma^{\rm AL}_{zz}(\widetilde{h}) = \frac{4e^2\xi_z^4}{\xi_x^2s^3}T^2_{c0}\tau^2_{\rm QF}(\widetilde{h}) = \frac{4e^2\xi_z^4}{\xi_x^2s^3}\left(\frac{\gamma_E}{\pi}\right)^2\frac{1}{\widetilde{h}^2}.$$

The negative contribution appearing from the diffusion coefficient renormalization competes with the positive $\delta\sigma^{\rm AL}_{zz}(\widetilde{h})$. The only difference between the in-plane [see Eqs. (7) and (12)] and $z$-axis components of this one-particle contribution consists of the anisotropy factor $\langle v_z^2\rangle/v_x^2 = \xi_z^2/\xi_x^2$. As a result, one gets

$$\delta\sigma^{\rm DCR}_{zz} = -\frac{2e^2}{3\pi^2 s}\frac{\xi_z^2}{\xi_x^2}\ln\frac{1}{\widetilde{h}}$$

and the total fluctuation correction to the $z$ axis magnetoconductivity at zero temperature above $H_{c2}(0)$ can be written as

$$\delta\sigma^{\rm (tot)}_{zz} = \frac{2e^2\xi_z^2}{3\pi^2\xi_x^2 s}\left[1.94\left(\frac{\xi_z}{s}\right)^2\frac{1}{\widetilde{h}^2} - \ln\frac{1}{\widetilde{h}}\right]. \qquad (15)$$

We used Eq. (15) for the analysis of unpublished data by M. Kartzovnik[26] on the magnetoresistance of the layered organic SC $\kappa-$(BEDT$-$TTF)$_2$Cu(NCS)$_2$ at low temperatures and magnetic fields above $H_{c2}(0)$. The measurement was taken at $T = 1.7$ K with a $T_{c0} \approx 9.5$ K and $B_{c2}(0) \approx 1.57$ T and this curve was fitted by $0.23(0.18/\widetilde{h}^2 + \ln\widetilde{h})$ (see Fig. 9). For the material parameters of this compound, the author reports $\tau = 1.7$ ps, $\xi_z = 0.3$–$0.4$ nm, and $s = 1$ nm. The fitting shown in Fig. 9 corresponds to the ratio $\xi_z/s = 0.32$ and looks rather convincing.

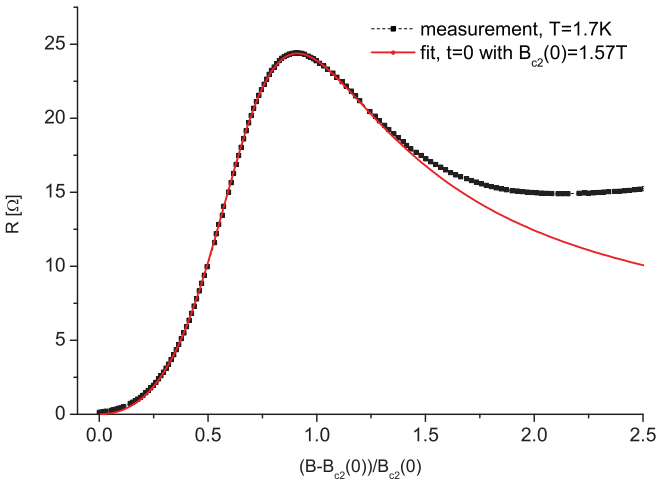


FIG. 9. (Color online) Comparison to resistivity measurements of the layered organic SC $\kappa-$(BEDT$-$TTF)$_2$Cu(NCS)$_2$ (Ref. 26). The material has a transition temperature of $T_{c0} \approx 9.5$ K, $B_{c2}(0) \approx 1.57$ T, and $\tau = 1.7$ ps. This experimental curve is taken at $T = 1.7$ K and fitted by expression in Eq. (15), which is in perfect agreement with the experiment. Specifics are given in the text.

The discrepancy appearing between the theoretical and experimental curves in the high field region, M. Kartsovnik attributes to the large normal-state magnetoresistance, reflecting the specifics of the cyclotron orbits on the multiconnected Fermi surface of the compound (due to the low crystal symmetry it is quite difficult to fit).

*Note added in proof.* Recently, we became aware of a report of an accurate experimental study of the SF contribution to conductivity depending on temperature and magnetic field—see Ref. 27. The authors carefully investigated superconducting fluctuations in the ab-plane conductivity above $T_c(H)$ in a series of doped $YBa_2Cu_3O_{6+x}$ samples from the deep pseudogap state to slight overdoping. For all doping values it is shown that the fluctuations are highly damped with increasing $T$ or $H$ and do not follow the standard Ginzburg-Landau approach. The data permitted to the authors define a line $H_c'(T)$ at which the SF contribution to conductivity becomes zero, as can be seen in our Figs. 2 and 3.


## ACKNOWLEDGMENTS

We thank T. Baturina, Yu. Galperin, M. Kartsovnik, A. Koshelev, B. Leridon, and M. Norman for useful discussions. The work was supported by the US Department of Energy Office of Science under the Contract No. DE-AC02-06CH11357. A.A.V. acknowledges support of the MIUR under the Project No. PRIN 2008 and the European Community FP7-IRSES programs ROBOCON and SIMTECH.

## APPENDIX A: ASLAMAZOV-LARKIN CONTRIBUTION

### 1. General expression

Let us start with the discussion of the AL contribution (diagram 1 in Fig. 1). The corresponding analytic expression is

$$Q_{xx}^{\mathrm{AL}}(\omega_\nu) = -4e^2T\sum_{\Omega_k}\sum_{\{n,m\}=0}^{\infty}\mathbf{B}_{nm}^{(x)}(\Omega_{k+\nu},\Omega_k)L_m(\Omega_k) \times B_{mn}^{(x)}(\Omega_k,\Omega_{k+\nu})L_n(\Omega_{k+\nu}). \tag{A1}$$

The block of three Green's functions $\mathbf{B}_{nm}$ with velocity operator (originating from the current vertex) and two Cooperons is given by

$$\mathbf{B}_{nm}(\Omega_{k+\nu},\Omega_k) = T\sum_{\varepsilon_i}\mathrm{Tr}\{G(\varepsilon_i)\widehat{\mathbf{v}}G(\varepsilon_{i+\nu})\widehat{\lambda}_n(\varepsilon_{i+\nu},\Omega_{k-i})G \times(\Omega_{k-i})\widehat{\lambda}_m(\Omega_{k-i},\varepsilon_i)\}. \tag{A2}$$

The trace operator Tr denotes the integration over all electron quantum numbers. The corresponding block was calculated in Ref. 15 exactly for fields with $\omega_c\tau \ll 1$, that is, for the case of our interest. Under this condition the Landau quantization affects the motion of Cooper pairs, while the Green's functions in the block Eq. (A2) can be used in $\tau$ approximation. As the result, using the properties of the velocity operator in Landau representation, one finds

$$B_{mn}^{(x)}(\Omega_{k+\nu},\Omega_k) = -2\nu_0\mathcal{D}[\sqrt{eH(n+1)}\delta_{m,n+1} + \sqrt{eHn}\delta_{m,n-1}]\Xi_{nm}(\Omega_{k+\nu},\Omega_k), \tag{A3}$$

with

$$\Xi_{nm}(\Omega_k,\Omega_{k+\nu}) = 2\pi T\sum_{\varepsilon_i}\frac{\Theta(-\varepsilon_{i+\nu}\Omega_{k-i})}{|2\varepsilon_i+\omega_\nu-\Omega_k|+\omega_c(n+1/2)} \times\frac{\Theta(-\varepsilon_i\Omega_{k-i})}{|2\varepsilon_i-\Omega_k|+\omega_c(m+1/2)}. \tag{A4}$$

Substituting Eq. (A3) in Eq. (A1) and further summation over Landau levels in Eq. (A1), results in the cancellation of the terms containing the products $\delta_{m,n+1}\delta_{n,m+1}$ and $\delta_{m,n-1}\delta_{n,m-1}$. The analysis of the $\theta$ functions in Eq. (A4) results in the possibility of separation of different domains of analyticity in the plane of bosonic frequencies $\Omega_k$:

$$\Xi_{mn}(\Omega_k,\Omega_k+\omega_\nu) = 2\pi T\left[\Theta(\Omega_k)\sum_{i=k}^{\infty}+\Theta(-\Omega_k)\sum_{i=0}^{\infty}+\Theta(-\Omega_k-\omega_\nu)\sum_{i=-\infty}^{k-1}+\Theta(\Omega_k+\omega_\nu)\sum_{i=-\infty}^{\nu-1}\right] \times\frac{1}{|2\varepsilon_i+\omega_\nu-\Omega_k|+\omega_c(n+1/2)}\frac{1}{|2\varepsilon_i-\Omega_k|+\omega_c(m+1/2)}. \tag{A5}$$

Summation over fermionic frequency in this expression can already be performed in terms of $\psi$ functions:

$$\Xi_{mn}(\Omega_k,\Omega_k+\omega_\nu) = \frac{1}{2\omega_c(n-m)}\left[\psi\left(\frac{1}{2}+\frac{\omega_\nu+|\Omega_k|+\omega_c(n+1/2)}{4\pi T}\right)-\psi\left(\frac{1}{2}+\frac{|\Omega_k|+\omega_c(m+1/2)}{4\pi T}\right) +\psi\left(\frac{1}{2}+\frac{|\Omega_{k+\nu}|+\omega_c(n+1/2)}{4\pi T}\right)-\psi\left(\frac{1}{2}+\frac{\omega_\nu+|\Omega_{k+\nu}|+\omega_c(m+1/2)}{4\pi T}\right)\right]. \tag{A6}$$

Being interested in the dc fluctuation conductivity, that is, taking into account the limit $\omega_\nu \to -i\omega \to 0$ after analytical continuation, in Eq. (A6) we neglected the frequency $\omega_\nu$ in comparison with $\omega_c(n-m)$ in the denominator since the diagonal term $(m=n)$ disappears in the process of summation over Landau levels in Eq. (A1) as follows from Eq. (A3). One notices the useful fact that the permutation $\Omega_k \Leftrightarrow \Omega_k+\omega_\nu$ simultaneously with $m \Leftrightarrow n$ in Eq. (A6) does not change the function $\Xi_{mn}(\Omega_k,\Omega_k+\omega_\nu)$:

$$\Xi_{mn}(\Omega_k,\Omega_k+\omega_\nu) \equiv \Xi_{nm}(\Omega_k+\omega_\nu,\Omega_k). \tag{A7}$$

Let us return to the general expression for paraconductivity Eq. (A1). One can transform the sum over the bosonic frequencies $\Omega_k$ to the contour integral $I^{\mathrm{AL}}$ in the plane of complex frequency $\Omega_k \to -iz$:

$$Q_{xx}^{\mathrm{AL}}(\omega_\nu) = -16e^2\nu_0^2\mathcal{D}^2eH\sum_{n,m}^{\infty}C_{mn}I_{nm}^{\mathrm{AL}}(\omega_\nu), \tag{A8}$$

$$I_{nm}^{\mathrm{AL}}(\omega_\nu) = \frac{1}{4\pi i}\oint\coth\left(\frac{z}{2T}\right)dz\,\Xi_{nm}(-iz+\omega_\nu,-iz) \times\Xi_{mn}(-iz,-iz+\omega_\nu)L_m(-iz)L_n(-iz+\omega_\nu), \tag{A9}$$

where the contour integral encloses all frequencies $\Omega_k$ [in the plane of frequency $z$ these are poles of $\coth(z/2T)$, see Fig. 10]. The coefficients

$$C_{mn} = (\delta_{m,n+1}\delta_{n,m-1}+\delta_{n,m+1}\delta_{m,n-1})\sqrt{n}\sqrt{(n+1)} \tag{A10}$$

control the summation over Landau levels.

Let us stress that both functions $\Xi$ in Eq. (A9) have breaks of their analyticity along the lines $\mathrm{Im}z=0$ and $\mathrm{Im}z=-\omega_\nu$, the same as the product of the propagators. As a result, one gets three domains where the integrand function is analytical: above the line $\mathrm{Im}z=0$, between the lines $\mathrm{Im}z=0$ and $\mathrm{Im}z=-\omega_\nu$, and below $\mathrm{Im}z=-\omega_\nu$. For the analytical continuation of function (A6) to the whole complex plane from Matsubara frequencies, three different functions: $\Xi_{nm}^{RR}$, $\Xi_{nm}^{RA}$, and $\Xi_{nm}^{AA}$, should be introduced, which are analytical in their corresponding domains. They differ by the combinations of the signs of the explicit absolute values appearing in Eq. (A6). Due to observation (A7) one can write the useful

identities

$$\Xi^{RR}_{nm}(-iz+\omega_\nu,-iz)=\Xi^{RR}_{mn}(-iz,-iz+\omega_\nu),$$
$$\Xi^{AA}_{nm}(-iz,-iz-\omega_\nu)=\Xi^{AA}_{mn}(-iz-\omega_\nu,-iz),$$
$$\Xi^{RA}_{nm}(-iz+\omega_\nu,-iz)=\Xi^{RA}_{mn}(-iz,-iz+\omega_\nu),$$

and get for the contour integral in Eq. (A9):

$$\begin{aligned}4\pi i I^{\mathrm{AL}}_{nm}(\omega_\nu)&=\int_{-\infty}^{\infty}\coth\left(\frac{z}{2T}\right)dz\Big\{\left[\Xi^{RR}_{nm}(-iz+\omega_\nu,-iz)\right]^2\\&\times L^R_m(-iz)-\left[\Xi^{RA}_{nm}(-iz+\omega_\nu,-iz)\right]^2L^A_m(-iz)\Big\}\\&\times L^R_n(-iz+\omega_\nu)+\int_{-\infty-i\omega_\nu}^{\infty-i\omega_\nu}\coth\left(\frac{z}{2T}\right)dz\\&\times\Big\{\left[\Xi^{RA}_{nm}(-iz+\omega_\nu,-iz)\right]^2L^R_n(-iz+\omega_\nu)\\&-\left[\Xi^{AA}_{nm}(-iz+\omega_\nu,-iz)\right]^2L^A_n(-iz+\omega_\nu)\Big\}L^A_m(-iz).\end{aligned}$$

The last integration can be reduced to that along the real axis by means of shifting the variable $-iz+\omega_\nu\to-iz'$. The resulting expression (A9) for the electromagnetic response operator—still defined on Matsubara frequencies $\omega_\nu$—takes the form

$$Q^{\mathrm{AL}}_{xx}(\omega_\nu)=4ie^2v_0^2\mathcal{D}^2\frac{eH}{\pi}\sum_{n,m}^{\infty}C_{mn}\times\int_{-\infty}^{\infty}\coth\left(\frac{z}{2T}\right)\Phi_{mn}(z,\omega_\nu)dz,\quad\text{(A11)}$$

where

$$\begin{aligned}\Phi_{mn}(z,\omega_\nu)&=\Big\{\left[\Xi^{RR}_{nm}(-iz+\omega_\nu,-iz)\right]^2L^R_m(-iz)-\left[\Xi^{RA}_{nm}(-iz+\omega_\nu,-iz)\right]^2L^A_m(-iz)\Big\}L^R_n(-iz+\omega_\nu)\\&+\Big\{\left[\Xi^{RA}_{mn}(-iz-\omega_\nu,-iz)\right]^2L^R_n(-iz)-\left[\Xi^{AA}_{nm}(-iz,-iz-\omega_\nu)\right]^2L^A_n(-iz)\Big\}L^A_m(-iz-\omega_\nu).\end{aligned}\quad\text{(A12)}$$

The rules for performing the analytical continuations of the function $\Xi_{mn}(\Omega_k,\Omega_k+\omega_\nu)$ in Eq. (A12) are simple: The sign of the explicitly written absolute values of the corresponding frequency in Eq. (A6) is chosen as "+" in the case of retarded continuation (superscript $R$) and it is chosen as "−" in the case of the advanced one (superscript $A$). For instance,

$$\begin{aligned}\Xi^{RA}_{mn}(\Omega_k,\Omega_k+\omega_\nu)=\frac{1}{2\omega_c(n-m)}\Bigg[&\psi\left(\frac{1}{2}+\frac{\omega_\nu-\Omega_k+\omega_c(n+1/2)}{4\pi T}\right)-\psi\left(\frac{1}{2}+\frac{-\Omega_k+\omega_c(m+1/2)}{4\pi T}\right)\\&+\psi\left(\frac{1}{2}+\frac{\omega_\nu+\Omega_k+\omega_c(n+1/2)}{4\pi T}\right)-\psi\left(\frac{1}{2}+\frac{2\omega_\nu+\Omega_k+\omega_c(m+1/2)}{4\pi T}\right)\Bigg],\end{aligned}$$

and analogously for $\Xi^{RR}_{nm}$ and $\Xi^{AA}_{nm}$.

Now one can perform the last analytical continuation $\omega_\nu\to-i\omega$ in Eq. (A12) and obtain $\Phi^{(R)}_{mn}(z,\omega)$ as an analytic function of the real external frequency $\omega$. Since we are interested in the dc limit of the FC, that is, $\omega\to0$, the function $\Phi^{(R)}_{mn}(z,\omega)$ can be presented in the form of its Taylor expansion:

$$\Phi^{(R)}_{mn}(z,\omega)=\Phi^{(R)}_{mn}(z,0)-\frac{i\omega}{\omega_c^2(n-m)^2}F_{nm}(-iz).$$

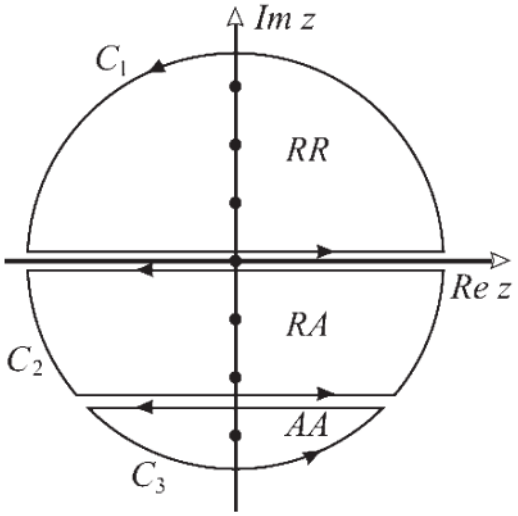


FIG. 10. The integration contour in the plane of complex frequencies.

The first term is not of interest here; all frequency independent contributions which form $Q^{(\mathrm{fl})}(0,T,H)$ are canceled out. This is a necessary requirement of the absence of the diamagnetic response in the normal phase of SCs. Actually, in order to find the FC we need to know only $\mathrm{Im}Q^{(\mathrm{fl})}(\omega,T,H)$; that is, we are interested only in the imaginary part of $F_{nm}(-iz)$. It can be obtained by expansion of all functions $\Xi^{\alpha\beta}_{nm}$ $(\alpha,\beta=R,A)$ and propagators in $\Phi^{(R)}_{mn}(z,\omega)$ over $\omega$. Introducing the function

$$\Psi_{nm}(iz)=\psi\left(\frac{1}{2}+\frac{iz+\omega_c(n+1/2)}{4\pi T}\right)-\psi\left(\frac{1}{2}+\frac{iz+\omega_c(m+1/2)}{4\pi T}\right)$$

one can find the analytically continued expressions for the products of Eq. (A12):

$$\left[\Xi^{RR}_{nm}\right]^2=\frac{\left[\Psi^2_{nm}(-iz)-\frac{i\omega}{2\pi T}\Psi_{nm}(-iz)\Psi'_{nm}(-iz)\right]}{\omega_c^2(n-m)^2},$$

$$\left[\Xi^{RA}_{mn}(-iz\pm i\omega,-iz)\right]^2=\frac{\mathrm{Re}\Psi_{nm}(-iz)}{\omega_c^2(n-m)^2}\times\left[\mathrm{Re}\Psi_{nm}(-iz)\pm\frac{i\omega}{4\pi T}\Psi'_{nm}(\pm iz)\right],$$

$$\left[\Xi^{AA}_{nm}\right]^2=\frac{1}{\omega_c^2(n-m)^2}\left[\Psi^2_{nm}(iz)+O(\omega^2)\right],$$

which leads to

$$\mathrm{Im}\Gamma_{nm}(-iz) = -\frac{\partial}{\partial z}\left\{2\mathrm{Re}\Psi^2_{nm}\mathrm{Im}L^R_m\mathrm{Im}L^R_n + \mathrm{Im}\Psi^2_{nm}\left[\mathrm{Im}L^R_n\mathrm{Re}L^R_m + \mathrm{Im}L^R_m\mathrm{Re}L^R_n\right]\right\}.$$

One can see that this function is symmetric with respect to subscripts permutation: $\mathrm{Im}\Gamma_{nm}(-iz) = \mathrm{Im}\Gamma_{mn}(-iz)$. Let us stress that we could present the linear in $\omega$ part of the function $\Phi^{(R)}_{mn}(z,\omega)$ in the form of full derivative with respect to $z$. The same situation was found in the original paper of Aslamazov and Larkin[2] for the simple case when the Green's functions block could be assumed to be constant. As a consequence of this important property of $\Phi^{(R)}_{mn}(z,\omega)$, the integration over $z$ in Eq. (A11) can be performed by parts. After summation over $m$, Eqs. (1) and (A8) read as

$$\delta\sigma^{\mathrm{AL}}_{xx}(T,H) = \frac{e^2}{2\pi T}\nu_0^2\sum_{n=0}^{\infty}(n+1)\int_{-\infty}^{\infty}\frac{dz}{\sinh^2(z/2T)} \times\left\{2\mathrm{Re}\Psi^2_{n,n+1}(-iz)\mathrm{Im}L^R_n(-iz)\mathrm{Im}L^R_{n+1}(-iz) + \mathrm{Im}\Psi^2_{n,n+1}(-iz)\left[\mathrm{Im}L^R_n(-iz)\mathrm{Re}L^R_{n+1}(-iz) + \mathrm{Im}L^R_{n+1}(-iz)\mathrm{Re}L^R_n(-iz)\right]\right\}. \quad \text{(A13)}$$

Let us attract attention to the fact that due to the integration by parts $\coth z/2T$ disappeared from the integral Eq. (A11) being replaced in Eq. (A13) by its derivative $\sinh^{-2}(z/2T)$. This fact makes our answer different from the one of Ref. 15 and physically means, as we see below, that at low temperatures the paraconducting contribution tends to zero: Fluctuation Cooper pairs above $H_{c2}(0)$ exist but do not move and do not participate directly in the charge transfer.[1,11]

It is convenient to introduce the dimensionless variable: $x = z/(2\pi T)$, parameters $t = T/T_{c0}$ and $h = 2e\xi^2 H$, where $\xi^2 = \pi\mathcal{D}/(8T)$, and the function

$$\mathcal{E}_m(t,h,ix) = \ln t + \psi\left[\frac{1+ix}{2} + \frac{2}{\pi^2}\left(\frac{h}{t}\right)(2m+1)\right] - \psi\left(\frac{1}{2}\right). \quad \text{(A14)}$$

In this representation, Eq. (A13) takes the form [$\mathcal{E}_k(t,h,ix) \equiv \mathcal{E}_k$]

$$\delta\sigma^{AL}_{xx}(t,h) = \frac{e^2}{\pi}\sum_{m=0}^{\infty}(m+1)\int_{-\infty}^{\infty}\frac{dx}{\sinh^2\pi x}\left\{\frac{[\mathrm{Re}^2(\mathcal{E}_m-\mathcal{E}_{m+1}) - \mathrm{Im}^2(\mathcal{E}_m-\mathcal{E}_{m+1})]\,\mathrm{Im}\,\mathcal{E}_m\,\mathrm{Im}\,\mathcal{E}_{m+1}}{|\mathcal{E}_m|^2|\mathcal{E}_{m+1}|^2} - \frac{\mathrm{Re}(\mathcal{E}_m-\mathcal{E}_{m+1})\,\mathrm{Im}(\mathcal{E}_m-\mathcal{E}_{m+1})(\mathrm{Im}\,\mathcal{E}_m\,\mathrm{Re}\,\mathcal{E}_{m+1} + \mathrm{Im}\,\mathcal{E}_{m+1}\,\mathrm{Re}\,\mathcal{E}_m)}{|\mathcal{E}_m|^2|\mathcal{E}_{m+1}|^2}\right\}. \quad \text{(A15)}$$

This is the general expression for fluctuation paraconductivity valid in all domains of temperatures and fields under consideration.

We see that all diagrams presented in Fig. 1 are relevant in different regions of the phase diagram, depicted in Fig. 5. Nine regions of different asymptotic behavior can be distinguished and below we analyze all contributions in each domain.

### 2. Asymptotic behavior

#### *a. Vicinity of $T_{c0}$, fields $h \ll 1[H \ll H_{c2}(0)]$*

In this case $\ln t = \epsilon \ll 1$ and the $\psi$ function in Eq. (A14) can be expanded. In the first approximation,

$$\mathcal{E}^{(1)}_m(t,h,ix) = \epsilon + \frac{i\pi^2 x}{4} + \left(\frac{2h}{t}\right)\left(m+\frac{1}{2}\right). \quad \text{(A16)}$$

The integral in Eq. (A15) can be easily carried out: Only the first fraction in the parentheses should be taken into account. Further summation over Landau levels can be performed exactly in terms of the $\psi$ function:

$$\delta\sigma^{\mathrm{AL}}_{xx}(\epsilon,h\ll 1) = \frac{e^2}{2\epsilon}\left(\frac{\epsilon}{2h}\right)^2\left[\psi\left(\frac{1}{2}+\frac{\epsilon}{2h}\right) - \psi\left(\frac{\epsilon}{2h}\right) - \frac{h}{\epsilon}\right], \quad \text{(A17)}$$

which coincides with the known expression for the Cooper pairs contribution to the magnetoconductivity in the GL region.[1]

The general Eq. (A15) makes it possible to obtain the next order correction in $\epsilon$ with respect to the AL result. In order to do this, one should take into account both terms and expand up to the second order:

$$\mathcal{E}^{(2)}_m(t,h,ix) = \mathcal{E}^{(1)}_m(t,h,ix) - \frac{14\zeta(3)\,ix}{\pi^2}\left(\frac{2h}{t}\right)\left(m+\frac{1}{2}\right) + 7\zeta(3)\frac{x^2}{4} - \frac{28\zeta(3)}{\pi^4}\left(\frac{2h}{t}\right)^2\left(m+\frac{1}{2}\right)^2. \quad \text{(A18)}$$

After some simple but cumbersome calculation in the limit of small fields, one finds

$$\delta\sigma^{\mathrm{AL}}_{xx}(\epsilon\ll 1) = \frac{e^2}{16\epsilon} - \frac{7\zeta(3)\,e^2}{8\pi^4}\ln\frac{1}{\epsilon}. \quad \text{(A19)}$$

In the first term one immediately recognizes the well-known 2D AL result. Nevertheless, our Eq. (A15) is obtained in a more general approach than the AL one,[2] since the former was derived accounting for the Green's functions block's $\Xi_{nm}(\Omega_k+\omega_\nu,\Omega_k)$ dependence on bosonic frequencies, which makes it possible to get the next order corrections in $\epsilon$. The second, logarithmic term in Eq. (A19) represents the next order correction with respect to the AL result in the vicinity of $T_{c0}$.

One can see that it is of the same kind as the DOS[5] and the regular MT[1] contributions (see below and Table I) but is 32 times smaller.

#### *b. High temperatures $T \gg T_{c0}$, weak fields $h \ll t$*

Let us move to the discussion of the high-temperature asymptotic. We assume $\ln t \gg 1$ in Eq. (A14) and get

$$\mathrm{Im}\mathcal{E}_m(t,h,ix) = \frac{x}{2}\psi'\left[\frac{1}{2} + \frac{4}{\pi^2}\left(\frac{h}{t}\right)(m+1/2)\right]. \tag{A20}$$

The sum in Eq. (A15) converges at $n_{\max} \sim t/h \gg 1$ and can be replaced by an integral. The integration over $x$ involves only the region $x \sim 1$ and can be performed first. As a result one gets

$$\delta\sigma_{xx}^{\mathrm{AL}}(t \gg 1, h \ll t) = \frac{e^2}{6\pi^2}\frac{C_1}{\ln^3 t},$$

with $C_1 = \frac{1}{3}\int_0^\infty [\psi'(1/2+x)]^3 dx = 6.97$. Let us stress that this asymptotic expression coincides with the high-temperature behavior of the AL contribution obtained in clean case[22] which emphasizes the statement that the 2D paraconductivity is a universal function of $\ln t$ throughout the complete temperature range.

#### *c. Fields close to the line $H_{c2}(T)$*

The line separating normal and superconducting phases $H_{c2}(T)$ [in our dimensionless units the line of critical fields $h_{c2}(t)$] is determined by the requirement that the propagator (2) has a pole when $\Omega_k = 0$ and $m = 0$:

$$\ln t + \psi\left(\frac{1}{2} + \frac{2}{\pi^2}\frac{h_{c2}(t)}{t}\right) - \psi\left(\frac{1}{2}\right) = 0.$$

At low temperatures $T \ll T_{c0}$, close to the point $T = 0$ and $H = H_{c2}(0)$, the critical field is $h_{c2}(t) = 2\xi^2 H_{c2}(0)/e \sim 1$. Then one can substitute the $\psi$ function by its asymptotic expression $\psi(x) = \ln x - 1/(2x)$ and take into account that $\psi(1/2) = -\ln 4\gamma_E$ ($\gamma_E = 1.781\ldots$ is the Euler's constant) which results in

$$h_{c2}(t \to 0) = \frac{\pi^2}{8\gamma_E}. \tag{A21}$$

In order to find the paraconducting contribution to FC above the curve $H_{c2}(T)$ in Fig. 5, let us rewrite Eq. (A14) in terms of the reduced field,

$$\widetilde{h}(t) = \frac{h - h_{c2}(t)}{h_{c2}(t)} \ll 1.$$

Below we see that the Cooper pair contribution to FC, which is singular in $\widetilde{h}^{-1}$, originates in Eq. (A15) only from the term with $m = 0$; that is, we can restrict ourselves to the LLL approximation. Hence, we need the explicit expression for $\mathcal{E}_m(t,\widetilde{h},ix)$ only for $m = 0,1$ and $\widetilde{h} \ll t \ll h_{c2}(t)$. In order to get this, one can use in Eq. (A14) a parametrization in terms of $\widetilde{h}$ and expand it $\widetilde{h} \ll 1$ and $h - h_{c2}(t) = \widetilde{h}\cdot h_{c2}(t) \ll t$. This gives

$$\mathcal{E}_0(t,\widetilde{h},ix) = \widetilde{h} + \frac{i\pi^2 x t}{4h_{c2}(t)}. \tag{A22}$$

The substitution of Eq. (A22) to Eq. (A15) results in

$$\delta\sigma_{xx}^{\mathrm{AL}}(t,h) = \frac{e^2}{\pi^2} J_{\mathrm{GL}}\left(\frac{4h_{c2}(t)\widetilde{h}}{\pi^2 t}\right), \tag{A23}$$

with

$$J_{\mathrm{GL}}(r) = \int_{-\infty}^{\infty}\frac{dx}{\sinh^2 x}\frac{x^2}{x^2+\pi^2 r^2} = 2r\psi'(r) - \frac{1}{r} - 2, \tag{A24}$$

first calculated in Ref. 15. This formula is valid along all the line $h_{c2}(t)$ until $t \sim h_{c2}(t)$. Taking into account the asymptotic expressions

$$\psi'(r\to\infty) = \frac{1}{r} + \frac{1}{2r^2} + \frac{1}{6r^3};\ \psi'(r\to 0) = 1/r^2, \tag{A25}$$

one finds that in this domain:

$$\delta\sigma_{xx}^{\mathrm{AL}}(t,h) = \begin{cases} \frac{4e^2\gamma_E^2 t^2}{3\pi^2\widetilde{h}^2}, & t \ll \widetilde{h}, \\ \frac{e^2 t}{4h_{c2}(t)\widetilde{h}}, & h_{c2}(t)\widetilde{h} \ll t. \end{cases} \tag{A26}$$

The first line of Eq. (A26) corresponds to the *QFs* which are realized in the limit of lowest temperatures $t \ll \widetilde{h}$ close to $H_{c2}(0)$. One sees that the paraconductivity decays here as $T^2$.

Let us underline the important difference between the first line of Eq. (A26) and the expression for the AL contribution obtained in Ref. 15 for the domain of QFs, where $t \ll \widetilde{h}$. The latter can be found in explicit form from Eqs. (9)–(11) of Ref. 15 in the limit $r = \widetilde{h}/(2\gamma_E t) \gg 1$:

$$\delta\sigma_{\mathrm{Ref.15}}^{\mathrm{AL}}(t \ll \widetilde{h}) = \frac{4e^2}{3\pi^2}\ln\frac{1}{\widetilde{h}} + \frac{16e^2\gamma_E^2 t^2}{9\pi^2\widetilde{h}^2}. \tag{A27}$$

The presence of the first, temperature-independent, term in Eq. (A27) obviously contradicts not only our result Eq. (A26), but also to the conclusions concerning the low-temperature behavior of the AL contribution of Refs. 11,12 and 17: In all these works $\delta\sigma_{AL}(t \ll \widetilde{h})$ decays with decreasing of temperature as $T^2$, while Eq. (A27) contains a temperature-independent term.

In the temperature range $h_{c2}(t)\widetilde{h} \ll t \ll h_{c2}(t)$ the paraconductivity is determined by the first line of Eq. (A26). Close to $H_{c2}(0)$ but for relatively high temperatures $t \sim \widetilde{h}$ the corresponding expression can be rewritten using the explicit expression for $h_{c2}(0)$ [Eq. (A21)]:

$$\delta\sigma_{xx}^{\mathrm{AL}}(t,h) = \frac{2\gamma_E e^2}{\pi^2}\left(\frac{t}{\widetilde{h}}\right), \tag{A28}$$

which perfectly matches to the first line of the Eq. (A26). Here the transition from quantum to classical fluctuations takes place. At higher temperatures along the line $h_{c2}(t)$ one should take into account the temperature dependence of $h_{c2}(t)$:

$$\delta\sigma_{xx}^{\mathrm{AL}}(t,h) = \frac{e^2}{4}\frac{t}{h - h_{c2}(t)}. \tag{A29}$$

This expression is valid along the line $h_{c2}(t)$ until $t \ll h_{c2}(t)$, where Eq. (A29) matches Eq. (A17).

#### *d. High fields [$H \gg H_{c2}(0)$], temperatures $t \ll h$*

In this domain we are far from the transition line $H_{c2}(T)$ [$h \gg h_{c2}(t)$] and the LLL approximation is not applicable. Nevertheless, one can substitute the summation over Landau levels by an integration. Replacing the digamma function, $\psi$, in Eq. (A14) by a logarithm, one finds that

$$\mathcal{E}_m(t,h,ix) = \ln\frac{4h}{\pi^2}\left(m+\frac{1}{2}\right) - \psi\left(\frac{1}{2}\right) + \frac{i\pi^2 xt}{4h(2m+1)}. \tag{A30}$$

One can see that this expression reproduces Eq. (A22) when $h \to h_{c2}(t)$ and $m = 0$. Let us substitute Eq. (A30) to Eq. (A15). As we see below, the sum converges at $m \sim 1$. It is why the main contribution comes from the second term of Eq. (A15), where the sum $\mathrm{Im}\mathcal{E}_m\mathrm{Re}\mathcal{E}_{m+1} + \mathrm{Im}\mathcal{E}_{m+1}\mathrm{Re}\mathcal{E}_m \sim \ln(\frac{4h}{\pi^2})$. As a result, we get

$$\delta\sigma_{xx}^{\mathrm{AL}}(t,h) = \frac{\pi^2 e^2}{192}\left(\frac{t}{h}\right)^2 \frac{C_2}{\ln^3\frac{2h}{\pi^2}},$$

with $C_2 = 0.545$. Let us recall that this expression is valid for arbitrary temperatures small in comparison to reduced field $t \ll h$.

## APPENDIX B: MAKI-THOMPSON CONTRIBUTION

### 1. General expression

Below we calculate the fluctuation renormalization of the one-electron contributions to conductivity. It is technically convenient to start with the usual expressions for the MT and other diagrams from Fig. 1, written in momentum representation. Only at the very end should one quantize the motion of Cooper pairs in a magnetic field in accordance with the rule

$$\frac{\mathcal{D}}{8T}\int\frac{d^2q}{(2\pi)^2} f[\mathcal{D}q^2] = \frac{h}{2\pi^2 t}\sum_{m=0}^{M} f\left[\omega_c(n+1/2)\right].$$

Diagram 2 of Fig. 1 can be written as

$$Q_{xx}^{\mathrm{MT}}(\omega_\nu) = 2e^2 T\sum_{\Omega_k}\int\frac{d^2\mathbf{q}}{(2\pi)^2} L(\mathbf{q},\Omega_k)\Sigma_{xx}^{\mathrm{MT}}(\mathbf{q},\Omega_k,\omega_\nu), \tag{B1}$$

where

$$\Sigma_{xx}^{\mathrm{MT}}(\mathbf{q},\Omega_k,\omega_\nu) = T\sum_{\varepsilon_n}\lambda(\mathbf{q},\varepsilon_{n+\nu},\Omega_{k-n-\nu}) \times \lambda(\mathbf{q},\varepsilon_n,\Omega_{k-n}) I_{xx}^{\mathrm{MT}}(\mathbf{q},\varepsilon_n,\Omega_k,\omega_\nu) \tag{B2}$$

and

$$I_{xx}^{\mathrm{MT}} = \int\frac{d^3\mathbf{p}}{(2\pi)^3} v_x(\mathbf{p})v_x(\mathbf{q}-\mathbf{p})G(\mathbf{p},\varepsilon_{n+\nu}) \times G(\mathbf{p},\varepsilon_n)G(\mathbf{q}-\mathbf{p},\Omega_{k-n-\nu})G(\mathbf{q}-\mathbf{p},\Omega_{k-n}).$$

The main $q$ dependence in (B1) arises from the propagator and vertices $\lambda$. That is why we can assume $q = 0$ in the Green's functions and calculate the electron momentum integral by changing, as usual, to a $\xi(\mathbf{p})$ integration:

$$I_{xx}^{\mathrm{MT}} = -\mathcal{D}\tau^{-1}\nu_0\int_{-\infty}^{\infty}\frac{d\xi}{\xi - i\widetilde{\varepsilon}_n}\frac{1}{\xi - i\widetilde{\varepsilon}_{n+\nu}} \times \frac{1}{\xi - i\widetilde{\Omega}_{k-n}}\frac{1}{\xi - i\widetilde{\Omega}_{k-n-\nu}}. \tag{B3}$$

This integral [Eq. (B3)] can be calculated using the Cauchy theorem. Closing the contour in the upper or lower half plane by the large semicircle and noticing that, due to fast decrease of the integrand the function in Eq. (B3), the integral over the semicircle becomes zero, one can express $J_{xx}$ in terms of the sum of the corresponding residues. There are six different combinations of the pole positions with respect to the real axis in the complex plane of $\xi$, leading to nonzero results (see Fig. 11): two realizations corresponding to $\theta(-\varepsilon_n\varepsilon_{n+\nu})\theta(\Omega_{k-n}\Omega_{k-n-\nu}) \neq 0$, one realization corresponding to $\theta(-\varepsilon_n\varepsilon_{n+\nu})\theta(-\Omega_{k-n}\Omega_{k-n-\nu}) \neq 0$, two realizations corresponding to $\theta(\varepsilon_n\varepsilon_{n+\nu})\theta(\Omega_{k-n}\Omega_{k-n-\nu}) \neq 0$, and the realization corresponding to $\theta(\varepsilon_n\varepsilon_{n+\nu})\theta(-\Omega_{k-n}\Omega_{k-n-\nu}) \neq 0$. Calculating the residues for each situation and assuming that $\widetilde{\varepsilon}_n = (2\tau)^{-1}\mathrm{sgn}\varepsilon_n$ (let us recall that we consider the disordered limit $T \ll \tau^{-1}$), one finds

$$\begin{aligned} I_{xx}^{\mathrm{MT}} = 2\pi\mathcal{D}\nu_0\tau^2 \{&\theta(-\varepsilon_n\varepsilon_{n+\nu})\,\theta(\Omega_{k-n}\Omega_{k-n-\nu}) \\ &+\theta(\varepsilon_n\varepsilon_{n+\nu})\,\theta(-\Omega_{k-n}\Omega_{k-n-\nu}) \\ &-2\theta(-\varepsilon_n\varepsilon_{n+\nu})\,\theta(-\Omega_{k-n}\Omega_{k-n-\nu}) \\ &-2\theta(\varepsilon_n\varepsilon_{n+\nu})\,\theta(\Omega_{k-n}\Omega_{k-n-\nu})\}. \end{aligned}$$

Now one should substitute this expression to Eq. (B2) and perform the summation over the fermionic frequencies. This is a cumbersome exercise, which, nevertheless, can be followed through analytically. Here we mention some useful transformations which are important to perform the summations: One can see that the simultaneous permutations $n \to -n$ and $k \to -k$ makes it possible to simplify the sums:

$$\begin{aligned} \Sigma_{xx}^{\mathrm{MT}} = \left(\Sigma_{xx}^{\mathrm{MT}(an)} + \Sigma_{xx}^{\mathrm{MT(reg2)}}\right) + \Sigma_{xx}^{\mathrm{MT(reg1)}} = -2\pi\nu_0\mathcal{D}T \\ \times\left\{\sum_{n=-\nu}^{-1}\frac{2\theta(-\Omega_{k-n}\Omega_{k-n-\nu}) - \theta(\Omega_{k-n}\Omega_{k-n-\nu})}{(|\varepsilon_{n+\nu} - \Omega_{k-n-\nu}| + \mathcal{D}q^2)(|\varepsilon_n - \Omega_{k-n}| + \mathcal{D}q^2)}\right. \\ \left. + 2\sum_{n=0}^{\infty}\frac{2\theta(\Omega_{k-n}\Omega_{k-n-\nu}) - \theta(-\Omega_{k-n}\Omega_{k-n-\nu})}{(|\varepsilon_{n+\nu} - \Omega_{k-n-\nu}| + \mathcal{D}q^2)(|\varepsilon_n - \Omega_{k-n}| + \mathcal{D}q^2)}\right\}. \end{aligned}$$

The rules writing the absolute values explicitly in the sum using the first $\theta$ function is evident. In the second sum, containing $\theta(\Omega_{k-n}\Omega_{k-n-\nu})$, one should make a shift $n' = n + \nu$. After rewriting the absolute values for the Cooperons, the sums can be expressed in terms of $\psi$ functions. Using the identity

$$\psi(1/2 + iz) - \psi(1/2 - iz) = \pi i\tanh\pi z$$

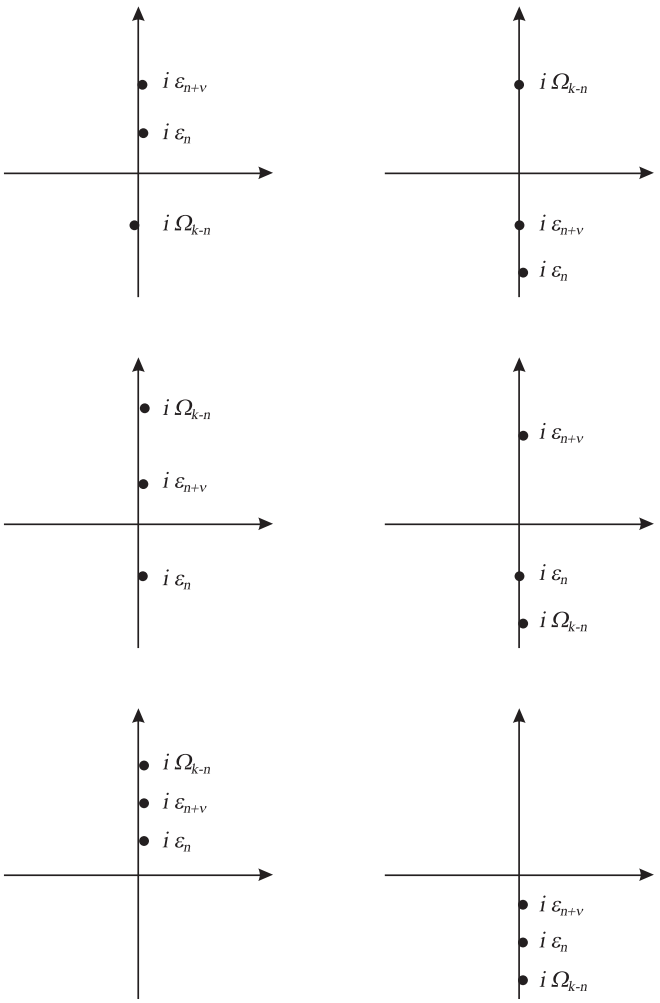


FIG. 11. $\xi$ integration in Eq. (B3). All six possible positions of the poles in the complex plane of $\xi$ are shown.

allows to write the final expression for the first sum as

$$\Sigma_{xx}^{\mathrm{MT(an)}}+\Sigma_{xx}^{\mathrm{MT(reg2)}} = -\frac{\mathcal{D}\nu_0\theta\left(\omega_{\nu-1}-|\Omega_k|\right)}{2(\omega_\nu+\mathcal{D}q^2)}\left[\psi\left(\frac{1}{2}+\frac{2\omega_\nu-|\Omega_k|+\mathcal{D}q^2}{4\pi T}\right) -\psi\left(\frac{1}{2}+\frac{|\Omega_k|+\mathcal{D}q^2}{4\pi T}\right)\right]. \tag{B4}$$

Looking at the denominator of this expression one can recognize that $\Sigma_{xx}^{\mathrm{MT(an)}}$ is responsible for the anomalous MT term.

Next we consider the remaining second sum in $\Sigma_{xx}^{\mathrm{MT}}$. One can see that in the first term both arguments of the absolute values are positive. In the second term we can replace $k\to -k$, with an additional change of the order of the summation over bosonic frequencies. The sum with $\theta\left(\Omega_{k-n}\Omega_{k-n-\nu}\right)$ can be calculated in the spirit of Eq. (B4). Regarding the last sum, containing $\theta\left(-\Omega_{k-n}\Omega_{k-n-\nu}\right)$, one can find that it is exactly equals to zero for any $\Omega_k$. Finally,

$$\Sigma_{xx}^{\mathrm{MT(reg1)}} = -\frac{\mathcal{D}\nu_0}{\omega_\nu}\left[\psi\left(\frac{1}{2}+\frac{2\omega_\nu+|\Omega_k|+\mathcal{D}q^2}{4\pi T}\right) -\psi\left(\frac{1}{2}+\frac{|\Omega_k|+\mathcal{D}q^2}{4\pi T}\right)\right]. \tag{B5}$$

Using the explicit Eqs. (B4) and (B5) we can perform the final summation over bosonic frequencies in Eq. (B1) and the analytical continuation of $Q_{xx}^{\mathrm{MT}}(\omega_\nu)$ to the axis of real frequencies. The analytical continuation of $Q_{xx}^{\mathrm{MT(reg1)}}$ is trivial since Eq. (B5) is the analytical function of $\omega_\nu$. As a result we get

$$Q_{xx}^{\mathrm{MT(reg1)R}}(\omega) = i\omega e^2\frac{\mathcal{D}\nu_0}{4\pi^2T}\int\frac{d^2\mathbf{q}}{(2\pi)^2} \times\sum_{k=-\infty}^{\infty}L(\mathbf{q},\Omega_k)\psi''\left(\frac{1}{2}+\frac{|\Omega_k|+\mathcal{D}q^2}{4\pi T}\right).$$

Next we go over from the integration over the momentum of the Cooper pair center of mass $\mathbf{q}$ to the summation over Landau levels. Recalling that the DOS at the Landau level is $H/\Phi_0$, one finds

$$\delta\sigma_{xx}^{\mathrm{MT(reg1)}} = \frac{e^2}{4\pi^2T}\frac{\mathcal{D}H}{\Phi_0}\sum_m\sum_{k=-\infty}^{\infty}\frac{4\mathcal{E}_m''(t,h,|k|)}{\mathcal{E}_m(t,h,|k|)}, \tag{B6}$$

where $\mathcal{E}_m^{(p)}(t,h,z)\equiv\partial_z^p\mathcal{E}_m(t,h,z)$; that is,

$$\mathcal{E}_m''(t,h,|k|) = \frac{1}{4}\psi''\left[\frac{1+|k|}{2}+\frac{2h}{\pi^2t}(2m+1)\right].$$

In the part of the electromagnetic operator related to Eq. (B4), the external frequency $\omega_\nu$ appears in the upper limit of the bosonic sum:

$$Q_{xx}^{\mathrm{MT(an)}}+Q_{xx}^{\mathrm{MT(reg2)}} = -2e^2T\mathcal{D}\nu_0\int\frac{d^2\mathbf{q}}{(2\pi)^2}\frac{1}{\omega_\nu+\mathcal{D}q^2}\sum_{|k|=0}^{\nu-1}L(\mathbf{q},\Omega_k) \times\left[\psi\left(\frac{1}{2}+\frac{2\omega_\nu-|\Omega_k|+\mathcal{D}q^2}{4\pi T}\right) -\psi\left(\frac{1}{2}+\frac{|\Omega_k|+\mathcal{D}q^2}{4\pi T}\right)\right],$$

and the procedure of analytical continuation is more sophisticated. First of all one can easily see that the contributions of positive and negative $k$ are equal. The method to continue such a sum the real frequencies was developed in Ref. 7 and consists in an Eliashberg transformation of the sum over $\Omega_k$ to an integral over the contour $\mathcal{C}$ (see Fig. 12 and the detailed description of this procedure in Ref. 1). One finds

$$Q_{xx}^{\mathrm{MT(an)}}+Q_{xx}^{\mathrm{MT(reg2)R}} = -4e^2T\mathcal{D}\nu_0\int\frac{d^2\mathbf{q}}{(2\pi)^2}\frac{1}{\omega_\nu+\mathcal{D}q^2} \times\left\{\frac{1}{2}L(\mathbf{q},0)\left[\psi\left(\frac{1}{2}+\frac{2\omega_\nu+\mathcal{D}q^2}{4\pi T}\right)-\psi\left(\frac{1}{2}+\frac{\mathcal{D}q^2}{4\pi T}\right)\right] +\frac{1}{2i}\oint_{C_2}dz\coth(\pi z)L(\mathbf{q},-iz)\left[\psi\left(\frac{1}{2}+\frac{2\omega_\nu+\mathcal{D}q^2}{4\pi T}+\frac{iz}{2}\right) -\psi\left(\frac{1}{2}+\frac{iz}{2}+\frac{\mathcal{D}q^2}{4\pi T}\right)\right]\right\}.$$

The residue at the point $z=i\nu$ is equal to zero. Shifting the variables in the integral over the upper line $\mathrm{Im}z=\nu$ as

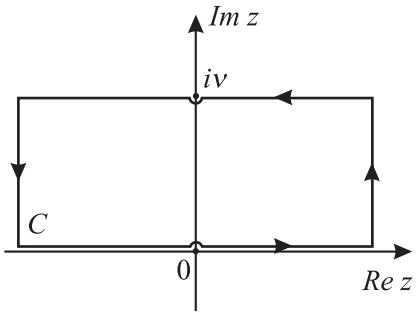


FIG. 12. Integration contour used in the analytic continuation of the MT contribution.

$z_1 = z' + i\nu$, one can present $Q_{xx}^{\mathrm{MT}}$ as an analytical function of $\omega_\nu$ and analytically continue it in the standard way $i\omega_\nu \to \omega \to 0$. Expanding it in small $\omega$ and integrating by parts, one gets

$$\delta\sigma_{xx}^{\mathrm{MT(an)}} + \delta\sigma_{xx}^{\mathrm{MT(reg2)}} = \frac{e^2}{2}\mathcal{D}\int\frac{d^2\mathbf{q}}{(2\pi)^2}\frac{1}{\tau_\phi^{-1}+\mathcal{D}q^2}\int_{-\infty}^{\infty}\frac{dz}{\sinh^2\pi z} \times \frac{\psi\left(\frac{1-iz}{2}+\frac{\mathcal{D}q^2}{4\pi T}\right)-\psi\left(\frac{1+iz}{2}+\frac{\mathcal{D}q^2}{4\pi T}\right)}{\ln\frac{T}{T_c}+\psi\left(\frac{1-iz}{2}+\frac{\mathcal{D}q^2}{4\pi T}\right)-\psi\left(\frac{1}{2}\right)}.$$

This expression is then transformed to the summations over Landau levels and written in the dimensionless variables, in the same way as was done before. Adding the regular part Eq. (B6), we finally write the most general expression for the MT contribution valid in all domains of temperature and magnetic field under consideration:

$$\begin{aligned}\delta\sigma^{\mathrm{MT}} &= \delta\sigma_{xx}^{\mathrm{MT(reg1)}} + \left(\delta\sigma_{xx}^{\mathrm{MT(an)}} + \delta\sigma_{xx}^{\mathrm{MT(reg2)}}\right)\\ &= \frac{e^2}{\pi^4}\left(\frac{h}{t}\right)\sum_{m=0}^{M}\left\{\sum_{k=-\infty}^{\infty}\frac{4\mathcal{E}_m''(t,h,|k|)}{\mathcal{E}_m(t,h,|k|)}+\frac{\pi^3}{\gamma_\phi+\frac{2h}{t}(m+1/2)}\right.\\ &\quad\left.\times\int_{-\infty}^{\infty}\frac{dz}{\sinh^2\pi z}\frac{\mathrm{Im}^2\,\mathcal{E}_m(t,h,iz)}{\mathrm{Re}^2\,\mathcal{E}_m(t,h,iz)+\mathrm{Im}^2\,\mathcal{E}_m(t,h,iz)}\right\},\end{aligned} \tag{B7}$$

where $M = (tT_{c0}\tau)^{-1}$ is the cutoff parameter.

### 2. Asymptotic behavior

#### *a. Contribution* $\delta\sigma_{xx}^{\mathrm{MT(reg1)}}$

Let us start with the evaluation of the contribution $\delta\sigma_{xx}^{\mathrm{MT(reg1)}}$ given by Eq. (B6).

*Vicinity of* $T_{c0}$*, fields* $h \ll 1 [H \ll H_{c2}(0)]$. Here one can just use Eq. (A14) for integer argument $k$, considering the smallness of $h/t$, expand the $\psi$ function, and perform the summation exactly:

$$\begin{aligned}&\delta\sigma_{xx}^{\mathrm{MT(reg1)}}(\epsilon \ll 1, h)\\ &\quad = -\frac{7\zeta(3)e^2}{\pi^4}\left[\psi\left(\frac{t}{2h}\right)-\psi\left(\frac{1}{2}+\frac{\epsilon t}{2h}\right)\right].\end{aligned} \tag{B8}$$

*High temperatures* $T \gg T_{c0}$*, weak fields* $h \ll t$. For the high-temperature asymptotic of Eq. (B6), we assume $\ln t \gg 1$. The sum over $k$ is determined by $\mathcal{E}_m''(t,h,|k|)$ and converges fast: It can be performed first. The remaining sum over Landau levels slowly diverges at large $m_{\max}$ and can be substituted by an integral. The double logarithmic divergence of this integral at the upper limit should be cut off at the limit corresponding $m_{\max} \sim (T_{c0}\tau)^{-1}$, which results in

$$\delta\sigma_{xx}^{\mathrm{MT(reg1)}} = -\frac{e^2}{\pi^2}\left[\ln\ln\frac{1}{T_{c0}\tau} - \ln\ln t\right]. \tag{B9}$$

One can see that close to $T_{c0}$ $\ln(\ln\ln t) \to \ln\left(\frac{1}{\epsilon}\right)$, Eqs. (B9) and (B8) therefore match each other.

*Fields close to the line* $H_{c2}(T)$. In this domain, as above, one can use the LLL approximation. Along the line $H_{c2}(T)$, in the region of classic fluctuations $\widetilde{h} \lesssim t \ll h_{c2}(t)$ the main contribution in Eq. (B6) gives the term with $k = 0$:

$$\delta\sigma_{xx}^{\mathrm{MT(reg1)}} = -\frac{e^2}{4}\frac{t}{h - h_{c2}(t)}. \tag{B10}$$

Close to $H_{c2}(0)$, but when still $t \gg \widetilde{h}$,

$$\delta\sigma_{xx}^{\mathrm{MT(reg1)}} = -\frac{2\gamma_E e^2}{\pi^2}\frac{t}{\widetilde{h}}. \tag{B11}$$

In the regime $t \lesssim \widetilde{h}$ the logarithmic term, appearing due to summation in Eq. (B6) over $k$ and corresponding to the contribution of the QFs, becomes of first importance:

$$\delta\sigma_{xx}^{\mathrm{MT(reg1)}} = -\frac{2e^2}{\pi^2}\ln\frac{1}{\widetilde{h}} - \frac{2\gamma_E e^2}{\pi^2}\frac{t}{\widetilde{h}}. \tag{B12}$$

*High fields* $H \gg H_{c2}(0)$*, temperatures* $t \ll h$. This domain is analogous to the previous one. As above, we first perform the summation over $k$ and integrate over Landau levels:

$$\delta\sigma_{xx}^{\mathrm{MT(reg1)}} = -\frac{e^2}{\pi^2}\left(\ln\ln\frac{1}{T_{c0}\tau} - \ln\ln\frac{2h}{\pi^2}\right). \tag{B13}$$

The only difference between Eqs. (B9) and (B13) consists of the lower limit: In the former it is determined by the temperature while in the latter its role is taken by the zero Landau level $\omega_c \gg T$. Equation (B13) is valid for arbitrary temperatures smaller $\omega_c$ and it obviously matches Eq. (B12) along the axis of the magnetic field ($t = 0$).

#### *b. Contribution* $\delta\sigma_{xx}^{\mathrm{MT(an)}} + \delta\sigma_{xx}^{\mathrm{MT(reg2)}}$

Now we consider the second part of the MT contribution Eq. (B7), namely, $\delta\sigma_{xx}^{\mathrm{MT(an)}} + \delta\sigma_{xx}^{\mathrm{MT(reg2)}}$.

*Vicinity of* $T_{c0}$*, fields* $h \ll 1 [H \ll H_{c2}(0)]$. In the vicinity of the critical temperature $T_{c0}$ one should use the expansion Eqs. (A16)–(A18) of $\mathcal{E}_m(t,h,ix)$. For the second-order correction it is sufficient to take on only the imaginary part of $\mathcal{E}_m(t,h,ix)$ into account. Substituting correspondingly $\mathrm{Re}\mathcal{E}_m^{(1)}(\epsilon,h \ll 1,ix)$ and $\mathrm{Im}\mathcal{E}_m^{(2)}(\epsilon,h \ll 1,ix)$ to Eq. (B7) and using the fact that $\gamma_\phi \ll 1$, the integral over $x$ can be easily performed [it converges for $x > x_0 \sim \epsilon + (\frac{h}{t})(2m+1)$]. The remaining summation is accomplished in terms of the $\psi$ functions and its result consists of two terms: The first one corresponds to the anomalous MT term $\delta\sigma_{xx}^{\mathrm{MT(an)}}$, while the second, $\delta\sigma_{xx}^{\mathrm{MT(reg2)}}$, exactly coincides in this region with

$\delta\sigma_{xx}^{\mathrm{MT(reg1)}}$ [Eq. (B10)]. Therefore, we present the total $\delta\sigma_{xx}^{\mathrm{MT}} = \delta\sigma_{xx}^{\mathrm{MT(reg1)}} + \delta\sigma_{xx}^{\mathrm{MT(an)}} + \delta\sigma_{xx}^{\mathrm{MT(reg2)}}$, which takes the form

$$\delta\sigma_{xx}^{\mathrm{MT}} = \frac{e^2}{8}\frac{1}{\epsilon-\gamma_\phi}\left[\psi\left(1/2+\frac{t\epsilon}{2h}\right)-\psi\left(1/2+\frac{t\gamma_\phi}{2h}\right)\right] - \frac{14\zeta(3)e^2}{\pi^4}\left[\ln\left(\frac{t}{2h}\right)-\psi\left(1/2+\frac{t\epsilon}{2h}\right)\right]. \quad \text{(B14)}$$

This formula is valid in the vicinity of the critical temperature $T_{c0}$, where we have three different regimes [weak fields $h \ll \epsilon$, GL strong fields $\epsilon \ll h$, and fields close to the $h_{c2}(\epsilon)$ line which is "mirrored" at $T_{c0}$].

*High temperatures $T \gg T_{c0}$, weak fields $h \ll t$.* Here we discuss the high-temperature asymptotic. As was done before, we assume $\ln t \gg 1$ and use Eqs. (A14) and (A20). Integration over $x$ due to the factor $\cosh^{-2}\pi z$ involves only the region $z \sim 1$ and can be performed first. The sum over Landau levels in this case converges at large $m_{\max} \sim t/h \gg 1$ and it can be substituted by an integral. The contributing part of the integration with logarithmic accuracy turns out to be only the fraction containing $\gamma_\phi$. As result we get

$$\delta\sigma_{xx}^{\mathrm{MT(an)}} + \delta\sigma_{xx}^{\mathrm{MT(reg2)}} = \frac{\pi^2 e^2}{192}\frac{\ln\frac{\pi^2}{2\gamma_\phi}}{\ln^2 t}. \quad \text{(B15)}$$

Despite the presence of the large logarithm $\ln\frac{\pi^2}{2\gamma_\phi}$ in this result in its numerator is relatively small with respect to Eq. (B9) due to the large $\ln^2 t$ in denominator of Eq. (B13).

*Fields close to the line $H_{c2}(T)$.* As was done in the case of the paraconductivity, let us use in Eq. (B7) the asymptotic Eq. (A22) and perform the calculations in the LLL approximation. One easily finds that the result in this case is also expressed in terms of the integral (A24):

$$\delta\sigma_{xx}^{\mathrm{MT(an)}} + \delta\sigma_{xx}^{\mathrm{MT(reg2)}} = \frac{e^2}{\pi^2}\frac{1}{1+t\gamma_\phi/h} J_{\mathrm{GL}}\left(\frac{4h_{c2}(t)}{\pi^2 t}\widetilde{h}\right). \quad \text{(B16)}$$

We consider the case of low temperatures $t \ll h_{c2}(t)$; hence, $\gamma_\phi \ll 1 \ll \frac{h}{t}$ and we can omit it in the denominator. In result it turns out that in this region Eq. (B16) exactly coincides with the corresponding AL contribution Eq. (A23). Therefore, it is determined by Eq. (A26) along the whole line $H_{c2}(T)$; that is, for $t \ll h_{c2}(t)$, which was already analyzed in detail above. Looking at Eqs. (A26) one can see that in the region $h - h_{c2}(t) \ll t$, strong cancellation takes place in the MT contribution $\delta\sigma_{xx}^{\mathrm{MT}}$ and only the logarithmic contribution remains

$$\delta\sigma_{xx}^{\mathrm{MT}} = -\frac{2e^2}{\pi^2}\ln\frac{2h_{c2}(t)}{\pi^2 t}.$$

In the regime of QFs $t \lesssim h - h_{c2}(t)$ the contribution $\delta\sigma_{xx}^{\mathrm{MT(an)}} + \delta\sigma_{xx}^{\mathrm{MT(reg2)}} \sim t^2$ and the linear (in $t$) part of $\delta\sigma_{xx}^{\mathrm{MT(reg1)}}$ are gradually frozen and the MT contribution reaches the finite negative value at zero temperature,

$$\delta\sigma_{xx}^{\mathrm{MT}} = -\frac{2e^2}{\pi^2}\ln\frac{1}{\widetilde{h}} - \frac{2\gamma_E e^2}{\pi^2}\frac{t}{\widetilde{h}(t)} + O\left[\left(\frac{t}{\widetilde{h}(t)}\right)^2\right].$$

*High fields $[H \gg H_{c2}(T)]$.* In this domain we are far from the transition line $H_{c2}(T)$ and the LLL approximation is not applicable. Replacing the $\psi$ function in the Eq. (A14) with the logarithm, one can use the asymptotic Eq. (A30) and get

$$\delta\sigma_{xx}^{\mathrm{MT(an)}} + \delta\sigma_{xx}^{\mathrm{MT(reg2)}} = \frac{7\zeta(3)\pi^2 e^2}{768}\frac{t^2}{h^2}\frac{1}{\ln^2\frac{2h}{\pi^2}},$$

which is beyond the accuracy of the large contribution $\delta\sigma_{xx}^{\mathrm{MT(reg1)}}$ [see Eq. (B13)] which, in result, determines the value of $\delta\sigma_{xx}^{\mathrm{MT}}$ in strong fields.

Finally, all asymptotic expressions for the MT diagram are summarized in Table III.

## APPENDIX C: DOS RENORMALIZATION: CONTRIBUTION OF THE DIAGRAMS 3–6

### 1. General expression

We start with calculation of diagram 4. As above, we use the intermediate results of Ref. 1 for the diagrams and then quantize the motion of the center of mass of the Cooper pair in magnetic field. The general expression for diagram 4 is given by

$$Q_{xx}^{(4)}(\omega_\nu) = 2e^2T^2\int\frac{d^2q}{(2\pi)^2}\sum_{k,n}L(q,\Omega_k)\lambda^2(q,\varepsilon_n,\Omega_{k-n})I_{xx}^{(4)}, \quad \text{(C1)}$$

with the integral $I_{xx}^{(4)}$ of the four electron Green's functions calculated exactly in Ref. 1 in the same spirit as demonstrated above:

$$\begin{aligned} I_{xx}^{(4)} &= \int\frac{d^2p}{(2\pi)^2}v_x^2G^2(p,\varepsilon_n)G(p,\varepsilon_{n+\nu})G(p,\Omega_{k-n}) \\ &= -2\pi\nu_0\mathcal{D}\tau^2\left[\Theta(\varepsilon_n\varepsilon_{n+\nu})\Theta(\varepsilon_n\varepsilon_{n-k}) + \Theta(-\varepsilon_n\varepsilon_{n+\nu})\Theta(-\varepsilon_n\varepsilon_{n-k})\right]. \end{aligned}$$

Substituting this expression to Eq. (C1) one finds

$$Q_{xx}^{(4)}(\omega_\nu) = -4\pi\nu_0\mathcal{D}e^2T^2\int\frac{d^2q}{(2\pi)^2}\sum_k L(q,|\Omega_k|) \times\left[2\sum_{n=0}^{\infty}\frac{\Theta(\varepsilon_n+\Omega_k)}{\left[2\varepsilon_n+\Omega_k+\mathcal{D}\mathbf{q}^2\right]^2} - \sum_{n=0}^{\nu-1}\frac{\Theta(\varepsilon_n+\Omega_k)}{[2\varepsilon_n+\Omega_k+\mathcal{D}\mathbf{q}^2]^2}\right]. \quad \text{(C2)}$$

The first term in this expression does not depend on external frequency and the corresponding part of the electromagnetic response operator does not contribute to conductivity. In the remaining part $\widetilde{Q}_{xx}^{(4)}(\omega_\nu)$ one can perform the summation over fermionic frequency and obtain it in the form of a sum of two terms:

$$\widetilde{Q}_{xx}^{(4,1)}(\omega_\nu) = \frac{\nu_0\mathcal{D}e^2}{4\pi}\int\frac{d^2q}{(2\pi)^2}\sum_{k=0}^{\infty}L(q,|\Omega_k|) \times\left[\psi'\left(\frac{1}{2}+\frac{\Omega_k+\mathcal{D}\mathbf{q}^2}{4\pi T}\right)-\psi'\left(\frac{1}{2}+\frac{2\omega_\nu+\Omega_k+\mathcal{D}\mathbf{q}^2}{4\pi T}\right)\right],$$

TABLE III. Asymptotic behavior of the MT contributions in different domains; see also Fig. 5 and Table II.

| Domain | $\delta\sigma_{xx}^{\mathrm{MT(an)}}+\delta\sigma_{xx}^{\mathrm{MT(reg2)R}}$ | $\delta\sigma_{xx}^{\mathrm{MT(reg1)}}$ | $\delta\sigma_{xx}^{\mathrm{MT}}$ |
|---|---|---|---|
| I | $\frac{e^2}{8}\frac{1}{\epsilon-\gamma_\phi}\ln\frac{\epsilon}{\gamma_\phi}-\frac{7\zeta(3)e^2}{\pi^4}\ln\left(\frac{1}{\epsilon}\right)$ | $-\frac{7\zeta(3)e^2}{\pi^4}\ln\frac{1}{\epsilon}$ | $\frac{e^2}{8}\frac{1}{\epsilon-\gamma_\phi}\ln\frac{\epsilon}{\gamma_\phi}-\frac{14\zeta(3)e^2}{\pi^4}\ln\left(\frac{1}{\epsilon}\right)$ |
| I–III | $\frac{e^2}{8}\frac{1}{\epsilon-\gamma_\phi}\left[\psi\left(1/2+\frac{t\epsilon}{2h}\right)-\psi\left(1/2+\frac{t\gamma_\phi}{2h}\right)\right]$ $-\frac{7\zeta(3)e^2}{\pi^4}\left[\ln\left(\frac{t}{2h}\right)-\psi\left(1/2+\frac{t\epsilon}{2h}\right)\right]$ | $-\frac{7\zeta(3)e^2}{\pi^4}\left[\psi\left(\frac{t}{2h}\right)-\psi\left(\frac{1}{2}+\frac{\epsilon t}{2h}\right)\right]$ | $\frac{e^2}{8}\frac{1}{\epsilon-\gamma_\phi}\left[\psi\left(1/2+\frac{t\epsilon}{2h}\right)-\psi\left(1/2+\frac{t\gamma_\phi}{2h}\right)\right]$ $-\frac{14\zeta(3)e^2}{\pi^4}\left[\ln\left(\frac{t}{2h}\right)-\psi\left(1/2+\frac{t\epsilon}{2h}\right)\right]$ |
| VII | $\frac{e^2}{4}\frac{t}{h-h_{c2}(t)}$ | $-\frac{e^2}{4}\frac{t}{h-h_{c2}(t)}-\frac{2e^2}{\pi^2}\ln\frac{2h}{\pi^2 t}$ | $-\frac{2e^2}{\pi^2}\ln\frac{2h}{\pi^2 t}$ |
| VI | $\frac{2\gamma_E e^2}{\pi^2}\frac{t}{h}$ | $-\frac{2\gamma_E e^2}{\pi^2}\frac{t}{h}-\frac{2e^2}{\pi^2}\ln\frac{2h}{\pi^2 t}$ | $-\frac{2e^2}{\pi^2}\ln\frac{2h}{\pi^2 t}$ |
| IV | $\frac{4e^2\gamma_E^2 t^2}{3\pi^2 h^2}$ | $-\frac{2\gamma_E e^2}{\pi^2}\frac{t}{h(t)}-\frac{2e^2}{\pi^2}\left[\ln\frac{1}{2h(t)}\right]$ | $-\frac{2e^2}{\pi^2}\left[\ln\frac{1}{2h}\right]-\frac{2\gamma_E e^2}{\pi^4}\frac{t}{h}$ |
| IX | $\frac{7\zeta(3)\pi^2 e^2}{768}\frac{t^2}{h^2}\ln^{-2}\frac{2h}{\pi^2}$ | $-\frac{e^2}{\pi^2}\left(\ln\ln\frac{1}{T_{c0}\tau}-\ln\ln\frac{2h}{\pi^2}\right)$ | $-\frac{e^2}{\pi^2}\left(\ln\ln\frac{1}{T_{c0}\tau}-\ln\ln\frac{2h}{\pi^2}\right)$ $+\frac{7\zeta(3)\pi^2 e^2}{768}\frac{t^2}{h^2}\ln^{-2}\frac{2h}{\pi^2}$ |
| VIII | $\frac{\pi^2 e^2}{192}\frac{\ln\frac{\pi^2}{2\gamma_\phi}}{\ln^2 t}$ | $-\frac{e^2}{\pi^2}\left[\ln\ln\frac{1}{T_{c0}\tau}-\ln\ln t\right]$ | $-\frac{e^2}{\pi^2}\left[\ln\ln\frac{1}{T_{c0}\tau}-\ln\ln t\right]+\frac{\pi^2 e^2}{192}\frac{\ln\frac{\pi^2}{2\gamma_\phi}}{\ln^2 t}$ |

$$\widetilde{Q}_{xx}^{(4,2)}(\omega_\nu)=\frac{\nu_0\mathcal{D}e^2}{4\pi}\int\frac{d^2q}{(2\pi)^2}\sum_{k=1}^{\nu-1}L\left(q,|\Omega_k|\right)$$
$$\times\left[\psi'\left(\frac{1}{2}+\frac{\Omega_k+\mathcal{D}\mathbf{q}^2}{4\pi T}\right)-\psi'\left(\frac{1}{2}+\frac{2\omega_\nu-\Omega_k+\mathcal{D}\mathbf{q}^2}{4\pi T}\right)\right].$$

The analytical continuation of the first one is trivial and it gives the first contribution to the conductivity, which in Landau representation takes the form

$$\delta\sigma_{xx}^{(4,1)}=\left(\frac{2e^2}{\pi^4}\right)\left(\frac{h}{t}\right)\sum_{m=0}^{M}\sum_{k=0}^{\infty}\frac{\mathcal{E}_m''(t,h,k)}{\mathcal{E}_m(t,h,k)}.$$

The analytical continuation of $\widetilde{Q}_{xx}^{(4,2)}(\omega_\nu)$ is completely analogous to that performed above in the case of the anomalous MT part. As a result, the total contribution of diagrams 3 and 4 can be presented as a sum of two very different terms

$$\delta\sigma_{xx}^{(3+4)}$$
$$=\frac{4e^2}{\pi^4}\left(\frac{h}{t}\right)\sum_{m=0}^{M}\left[\sum_{k=0}^{\infty}\frac{\mathcal{E}_m''(t,h,k)}{\mathcal{E}_m(t,h,k)}\right.$$
$$\left.+\frac{\pi}{2}\int_{-\infty}^{\infty}\frac{dx}{\sinh^2(\pi x)}\frac{\mathrm{Im}\,\mathcal{E}_m(t,h,ix)\,\mathrm{Im}\,\mathcal{E}_m'(t,h,ix)}{\mathrm{Re}^2\,\mathcal{E}_m(t,h,ix)+\mathrm{Im}^2\,\mathcal{E}_m(t,h,ix)}\right]. \quad \text{(C3)}$$

Next we discuss diagram 5. Its contribution can be written in the same way as above:

$$Q_{xx}^{(5)}(\omega_\nu)=\frac{e^2T^2v_F^2}{2\pi\nu_0\tau}\int\frac{d^2q}{(2\pi)^2}\sum_{n,k}L\left(q,\Omega_k\right)\lambda^2\left(q,\varepsilon_n,\Omega_{k-n}\right)$$
$$\times I^{(5)}\left(\varepsilon_n,\varepsilon_{n+\nu}\right)I^{(5)}\left(\varepsilon_n,-\varepsilon_{n-k}\right),$$

where the integral

$$I^{(5)}\left(\varepsilon_n,\varepsilon_{n+\nu}\right)=\int\frac{d^2p}{(2\pi)^2}G^2\left(p,\varepsilon_n\right)G\left(p,\varepsilon_{n+\nu}\right)$$
$$=2\pi i\nu_0\tau^2\mathrm{sgn}\varepsilon_{n+\nu}\Theta\left(-\varepsilon_{n+\nu}\varepsilon_n\right). \quad \text{(C4)}$$

As a result:

$$Q_{xx}^{(5)}(\omega_\nu)=-4\pi\nu_0\mathcal{D}e^2T^2\int\frac{d^2q}{(2\pi)^2}\sum_{k=-\infty}^{\infty}L\left(q,\Omega_k\right)$$
$$\times\sum_{n=-\nu}^{-1}\frac{\Theta\left(\Omega_k-\varepsilon_n\right)}{\left[|2\varepsilon_n-\Omega_k|+\mathcal{D}\mathbf{q}^2\right]^2}. \quad \text{(C5)}$$

Further evaluation of this expression is very similar to that one of $\widetilde{Q}_{xx}^{(5)}(\omega_\nu)$. In particular, after summation over fermionic frequencies, $Q_{xx}^{(7)}(\omega_\nu)$ is presented in the form of two sums over bosonic frequencies: one in the limits $k\in[0,\infty)$, the other $k\in[1,\nu-1]$, and following step by step the same procedure of the analytical continuation as before, one finds that $\delta\sigma_{xx}^{(5,1)}=-\delta\sigma_{xx}^{(4,1)}$ and $\delta\sigma_{xx}^{(5,2)}=\delta\sigma_{xx}^{(4,2)}$. Therefore, we get

$$\delta\sigma_{xx}^{(5+6)}=\frac{4e^2}{\pi^4}\left(\frac{h}{t}\right)\sum_{m=0}^{M}\left[-\sum_{k=0}^{\infty}\frac{\mathcal{E}_m''(t,h,k)}{\mathcal{E}_m(t,h,k)}+\frac{\pi}{2}\int_{-\infty}^{\infty}\frac{dx}{\sinh^2(\pi x)}\right.$$
$$\left.\times\frac{\mathrm{Im}\mathcal{E}_m(t,h,ix)\,\mathrm{Im}\mathcal{E}_m'(t,h,ix)}{\mathrm{Re}^2\mathcal{E}_m(t,h,ix)+\mathrm{Im}^2\mathcal{E}_m(t,h,ix)}\right]. \quad \text{(C6)}$$

Evaluating the sum and integral close to $T_{c0}$ one can see that the first term in Eq. (C3) is twice larger than the second one. Comparing Eq. (C3) to Eq. (C6) we obtain the old result: $3\delta\sigma_{xx}^{(5+6)}=-\delta\sigma_{xx}^{(3+4)}$ (Ref. 9), used later in Refs. 1,5,6,15. However, it is necessary to stress that the last statement *is not universal:* Far from the critical temperature, or at low temperatures, close to $H_{c2}(0)$, the integrals in Eqs. (C3)–(C6) are small with respect to the contribution of the sums. Regarding the latter, they enter in Eqs. (C3)–(C6) with the opposite sign. After the summation in $\delta\sigma_{xx}^{(5-8)}$ these just cancel each other (in this region of temperatures $\delta\sigma_{xx}^{(3+4)}\approx-\delta\sigma_{xx}^{(5+6)}$). To avoid misunderstanding,[15] it is more convenient to use the total contribution of the DOS-like diagrams 3–6 in the form:

$$\delta\sigma_{xx}^{(\mathrm{DOS})}=\frac{4e^2}{\pi^3}\frac{h}{t}\sum_{m=0}^{M}\int_{-\infty}^{\infty}\frac{dx}{\sinh^2\pi x}$$
$$\times\frac{\mathrm{Im}\,\mathcal{E}_m(t,h,ix)\,\mathrm{Im}\,\mathcal{E}_m'(t,h,ix)}{\mathrm{Re}^2\,\mathcal{E}_m(t,h,ix)+\mathrm{Im}^2\,\mathcal{E}_m(t,h,ix)}. \quad \text{(C7)}$$

### 2. Asymptotic behavior

#### *a. Vicinity of $T_{c0}$, fields $h \ll 1[H \ll H_{c2}(0)]$*

In this case $\ln t = \epsilon \ll 1$, the $\psi$ function in Eq. (A14) can be expanded. The function $\mathcal{E}_m(t,h,ix)$ is determined by Eq. (A16). Its substitution to Eq. (C7) results in

$$\delta\sigma_{xx}^{\mathrm{DOS}} = -\frac{14\zeta(3)e^2}{\pi^4}\left[\ln(1/2h) - \psi\left(1/2+\frac{\epsilon}{2h}\right)\right] = -\frac{14\zeta(3)e^2}{\pi^4}\begin{cases}\ln(1/\epsilon), & h \ll \epsilon,\\ \ln\left(\frac{1}{2h}\right), & \epsilon \ll h \ll 1.\end{cases} \tag{C8}$$

This expression is valid in the vicinity of the critical temperature $T_{c0}$ and exactly reproduces existing results.[5,6]

#### *b. High temperatures, high fields*

Next we discuss the high-temperature asymptotic. As was done above, we assume $\ln t \gg 1$ and use Eqs. (A14)–(A20). The sum over Landau levels in this case converges at large $m_{\max} \sim t/h \gg 1$ and can be substituted by an integral. The main integral contribution comes only from the region up to $x \sim 1$ and can be performed first. One gets

$$\delta\sigma_{xx}^{\mathrm{DOS}} = -\frac{\pi^2 e^2}{192\ln^2 t}. \tag{C9}$$

We see that this result differs from that one of Ref. 9. The cancellation of the sums of Eqs. (C3)–(C6) in $\delta\sigma_{xx}^{\mathrm{DOS}}$ removes the double logarithmic term $\ln\ln t$ from it. Nevertheless, such terms in $\delta\sigma_{xx}^{(\mathrm{tot})}$ still appear from the regular MT term and, as we see below, from diagrams 9 and 10.

In the limit of high fields $h \gg t$ the summation over Landau levels gives

$$\delta\sigma_{xx}^{\mathrm{DOS}} = -\frac{7\zeta(3)\pi^2 e^2}{384}\left(\frac{t}{h}\right)^2 \frac{1}{\ln^2\frac{2h}{\pi^2}}.$$

#### *c. Above the line $H_{c2}(T)$ but $t \ll h_{c2}(t)$*

Using the asymptotic Eq. (A22) one can perform the integration in Eq. (C7) and express $\delta\sigma_{xx}^{\mathrm{DOS}}$ in terms of the integral $J_{\mathrm{GL}}$:

$$\delta\sigma_{xx}^{\mathrm{DOS}} = -\frac{e^2}{\pi^2}\sum_{m=0}^{M}\frac{J_{\mathrm{GL}}\left[\frac{4h(2m+1)}{\pi^2 t}\ln\frac{4h}{\pi^2}\left(m+\frac{1}{2}\right)\right]}{(2m+1)}.$$

Close to the line $H_{c2}(T)$ we can restrict ourselves to the LLL and immediately get

$$\delta\sigma_{xx}^{(\mathrm{DOS})} = -\frac{e^2}{\pi^2}J_{\mathrm{GL}}\left(\frac{4\widetilde{h}}{\pi^2 t}\right).$$

Looking on the asymptotic behavior of $J(r)$ at low temperatures, one notices that, in contrast to the statement of Ref. 15, the group of diagrams 5–8 does not give any contribution to $\delta\sigma_{xx}^{(\mathrm{tot})}$ when temperature tends to zero. Nevertheless, a nontrivial contribution of QFs $\sim \ln\widetilde{h}$, found in Ref. 15, exists due to the regular MT term and diagrams 9 and 10.

## APPENDIX D: RENORMALIZATION OF THE DIFFUSION COEFFICIENT: CONTRIBUTION OF DIAGRAMS 7–10

### 1. General expression

We start with the calculation of diagram 7:

$$Q_{xx}^{(7)}(\omega_\nu) = 2e^2T^2\sum_{k,n}\int\frac{d^2q}{(2\pi)^2}L(q,\Omega_k)\,\lambda(\mathbf{q},\varepsilon_n,\Omega_k-\varepsilon_n) \times\lambda(\mathbf{q},\varepsilon_{n+\nu},\Omega_k-\varepsilon_{n+\nu}) \times C(q,\varepsilon_{n+\nu},\Omega_k-\varepsilon_n)\,I_1^{(7)}I_2^{(7)}, \tag{D1}$$

where the integrals of the Green's function products can be calculated in the standard way:

$$I_{(1)}^{(7)}(\varepsilon_n,\varepsilon_{n+\nu},\Omega_{k-n}) = \int\frac{d^Dp}{(2\pi)^D}v_x(p)G(p,\varepsilon_n)G(p,\varepsilon_{n+\nu})G(q-p,\Omega_{k-n}) = 4\pi\nu_0\mathcal{D}\mathbf{q}_x\tau^2\theta(\varepsilon_n\varepsilon_{n+\nu})\theta(-\varepsilon_n\Omega_{k-n}),$$
$$I_{(2)}^{(7)} = I_{(1)}^{(7)}(\Omega_{k-n-\nu},\Omega_{k-n},\varepsilon_{n+\nu}). \tag{D2}$$

Substitution of these expressions to Eq. (D1) and accounting for the fact that $\overline{\mathcal{D}\mathbf{q}_x^2} = \mathcal{D}\mathbf{q}^2/2$ results in

$$Q_{xx}^{(7)} = 8\pi\nu_0\mathcal{D}e^2T^2\int\frac{\mathcal{D}\mathbf{q}^2d^2q}{(2\pi)^2}\sum_{k=-\infty}^{\infty}L(q,\Omega_k) \times\sum_{n=-\infty}^{\infty}\frac{\theta[-\varepsilon_n(\Omega_k-\varepsilon_n)]}{|2\varepsilon_n-\Omega_k|+\mathcal{D}\mathbf{q}^2} \times\frac{\theta[-\varepsilon_{n+\nu}(\Omega_k-\varepsilon_{n+\nu})]}{|2\varepsilon_{n+\nu}-\Omega_k|+\mathcal{D}\mathbf{q}^2}\frac{\theta(\varepsilon_n\varepsilon_{n+\nu})}{|2\varepsilon_n+\omega_\nu-\Omega_k|+\mathcal{D}\mathbf{q}^2}.$$

The $\theta-$function $\theta(\varepsilon_n\varepsilon_{n+\nu})$ defines the limits of summation over fermionic frequencies $n$ as $(-\infty,-\nu-1]$ and $[0,\infty)$. Changing the sign of summation in the first interval and then shifting the variable of summation $\varepsilon_n+\omega_\nu\to\varepsilon_{n'}$, one finds that the expression is even in $\Omega_k$, which makes it possible to present $Q_{xx}^{(7)}(\omega_\nu)$ in the form of an analytical function of $\omega_\nu$, to perform the analytical continuation $\omega_\nu\to-i\omega$, and to expend it over small $\omega$:

$$Q_{xx}^{(7)R}(\omega) = -8\pi\nu_0\mathcal{D}e^2T^2\sum_{k=-\infty}^{\infty}\int\mathcal{D}\mathbf{q}^2L(q,\Omega_k)\frac{d^2q}{(2\pi)^2} \times\sum_{n=0}^{\infty}\left\{\frac{1}{[2\varepsilon_n+|\Omega_k|+\mathcal{D}\mathbf{q}^2]^3} + \frac{3i\omega}{[2\varepsilon_n+|\Omega_k|+\mathcal{D}\mathbf{q}^2]^4}\right\}. \tag{D3}$$

The corresponding contribution to the conductivity is determined by the imaginary part of Eq. (D3). Quantizing the motion of Cooper pairs and going over to the Landau representation, one finds

$$\delta\sigma_{xx}^{(7+8)} = \frac{2e^2}{\pi^6}\left(\frac{h}{t}\right)^2\sum_{m=0}^{M}\left(m+\frac{1}{2}\right)\sum_{k=-\infty}^{\infty}\frac{8\mathcal{E}_m'''(t,h,|k|)}{\mathcal{E}_m(t,h,|k|)}. \tag{D4}$$

Comparing this formula with Eq. (B7) one can see that beyond the vicinity of $T_{c0}$ the contribution of diagrams 7 and 8 given

by the Eq. (D4) cancels the regular MT contribution [given by the first term of Eq. (B7)].

Finally, we proceed with the calculation of diagram 9. Two integrals of the three Green's function blocks in it are equal and coincide with $I_1^{(7)}$. Substituting Eq. (D2) to the general expression for $Q_{xx}^{(9)}(\omega_\nu)$ and performing the summation over fermionic frequencies in the spirit of the above calculations, one finds

$$Q_{xx}^{(9)}(\omega_\nu) = -\frac{e^2T}{4\pi^2\nu_0\tau^4\omega_\nu^2}\sum_{k=-\infty}^{\infty}\int\frac{d^2q}{(2\pi)^2}\mathcal{D}\mathbf{q}^2L(q,\Omega_k) \times[\Psi_1(|\Omega_k|,\omega_\nu)-\Psi_2(|\Omega_{k+\nu}|,\omega_\nu)] = Q_{(1)}^{(9)}+Q_{(2)}^{(9)}, \tag{D5}$$

where

$$\Psi_\gamma(x,\omega_\nu)=\left[\psi\left(\frac{1}{2}+\frac{\omega_\nu+x+\mathcal{D}\mathbf{q}^2}{4\pi T}\right)-\psi\left(\frac{1}{2}+\frac{x+\mathcal{D}\mathbf{q}^2}{4\pi T}\right) -\frac{\omega_\nu}{(4\pi T)}\psi'\left(\frac{1}{2}+\frac{\omega_\nu}{4\pi T}\delta_{\gamma 2}+\frac{x+\mathcal{D}\mathbf{q}^2}{4\pi T}\right)\right], \tag{D6}$$

with $\gamma = 1,2$ and Kronecker $\delta_{ij}$.

There is no problem to perform analytical continuation of the first term of Eq. (D5): The function $\Psi_1(|\Omega_k|,\omega_\nu)$ is analytical in its argument $\omega_\nu$, and the corresponding contribution to Eq. (D5) can be continued in the standard way $\omega_\nu \to -i\omega \to 0$. Expanding Eq. (D6) with $\gamma = 1$ over $\omega$ one finds the essential contribution to the electromagnetic response operator:

$$Q_{(1)}^{(9)R}(\omega) = -i\omega\frac{\mathcal{D}\nu_0e^2T}{3(4\pi T)^3}\sum_{k=-\infty}^{\infty}\int\mathcal{D}\mathbf{q}^2\frac{d^2q}{(2\pi)^2} \times L(q,\Omega_k)\psi'''\left(\frac{1}{2}+\frac{|\Omega_k|+\mathcal{D}\mathbf{q}^2}{4\pi T}\right). \tag{D7}$$

The evaluation of the second term of Eq. (D5) turns out to be much more sophisticated, since $\omega_\nu$ appears in $\Psi_2(|\Omega_{k+\nu}|,\omega_\nu)$ not only as parameter but also in the argument $|\Omega_{k+\nu}|$ of this nonanalytical function. The situation is analogous to the AL contribution and the same method of analytical continuation has to be applied. The corresponding sum over bosonic frequencies is transformed in an integral over the contour $\mathcal{C}$ shown in Fig. 10 with three regions of different analytic behavior:

$$Q_{(2)}^{(9)}(\omega_\nu) = \frac{1}{2\pi i}\frac{\mathcal{D}\nu_0e^2}{\omega_\nu^2}\int\mathcal{D}\mathbf{q}^2\frac{d^2q}{(2\pi)^2} \times\oint_C\coth\frac{z}{2T}L(q,-iz)\psi_1(|\Omega_{k+\nu}|,\omega_\nu).$$

After shifting of the variable $z$ of the integral over the line $\mathrm{Im}z = -\omega_\nu$ as $-iz+\omega_\nu \to -iz'$, one gets $Q_{(2)}^{(9)}(\omega_\nu)$ already as an analytical function of $\omega_\nu$:

$$Q_{(2)}^{(9)}(\omega_\nu) = \frac{\mathcal{D}\nu_0e^2}{\pi\omega_\nu^2}\int\mathcal{D}\mathbf{q}^2\frac{d^2q}{(2\pi)^2}\int_{-\infty}^{\infty}dz\coth\left(\frac{z}{2T}\right) \times\left[\Psi_2^R(-iz+\omega_\nu,\omega_\nu)\mathrm{Im}L^R(q,-iz) + L^A(q,-iz-\omega_\nu)\,\mathrm{Im}\Psi_2^R(-iz,\omega_\nu)\right]. \tag{D8}$$

Obviously, this expression can be continued in $\omega_\nu$ in the standard way $\omega_\nu \to -i\omega$.

We are interested in the imaginary part of $Q_{(2)}^{(9)R}(\omega)$; that is, only $\mathrm{Im}\Psi_2^R(-iz-i\omega,-i\omega)$ and $\mathrm{Im}\Psi_2^R(-iz,-i\omega)$ are essential. They can be can be written explicitly from Eq. (D6):

$$\mathrm{Im}\Psi_2^R(-iz,-i\omega) = -\frac{\omega^3}{3(4\pi T)^4}\mathrm{Re}\psi'''\left(\frac{1}{2}+\frac{-iz+\mathcal{D}\mathbf{q}^2}{4\pi T}\right), \tag{D9}$$

with $\mathrm{Im}\Psi_2^R(-iz-i\omega,-i\omega) = 5\mathrm{Im}\Psi_2^R(-iz,-i\omega)$. Since we are interested only in the linear $\omega$ part of $\mathrm{Im}Q_{(2)}^{(9)R}(\omega)$ in the analytically continued Eq. (D8), one can omit $i\omega$ in the argument of $L^A(q,-iz+i\omega)$ and recall that $\mathrm{Im}L^A(q,-iz) = -\mathrm{Im}L^R(q,-iz)$. One gets

$$\mathrm{Im}Q_{(2)}^{(9)}(\omega) = \frac{4\omega\mathcal{D}\nu_0e^2}{3\pi(4\pi T)^4}\int\mathcal{D}\mathbf{q}^2\frac{d^2q}{(2\pi)^2}\int_{-\infty}^{\infty}dz\coth\left(\frac{z}{2T}\right) \times\mathrm{Re}\psi'''\left(\frac{1}{2}+\frac{-iz+\mathcal{D}\mathbf{q}^2}{4\pi T}\right)\mathrm{Im}L^R(q,-iz).$$

Now one can see that the integrand function is odd in $z$ and its integration with symmetric limits gives zero. Hence, in linear approximation $\mathrm{Im}Q_{(2)}^{(9)}(\omega) = 0$ and the second term of Eq. (D5) does not contribute to conductivity. Going over to the dimensionless variables in Eq. (D7) and to the Landau representation, one finds that $\delta\sigma_{xx}^{(9)} = -\delta\sigma_{xx}^{(7)}/3$. Finally, the total contribution of diagrams 7–10, determining the renormalization of the one-particle diffusion coefficient in the presence of SFs, is

$$\delta\sigma_{xx}^{7-10} = \frac{4e^2}{3\pi^6}\left(\frac{h}{t}\right)^2\sum_{m=0}^{M}\sum_{k=-\infty}^{\infty}\left(m+\frac{1}{2}\right)\frac{8\mathcal{E}_m'''(t,h,|k|)}{\mathcal{E}_m(t,h,|k|)}. \tag{D10}$$

### 2. Asymptotic behavior

#### *a. Vicinity of $T_{c0}$, fields $h \ll 1[H \ll H_{c2}(0)]$*

In contrast to the AL, MT, and DOS contributions, due to presence of the multiplier $\mathcal{D}\mathbf{q}^2$ in the numerator of Eq. (D5) [corresponding to $(m+\frac{1}{2})$ in Eq. (D10) close to the critical temperature $T_{c0}$], the value $\delta\sigma_{(2)}^{\mathrm{DCR}}$ turns out to be not singular in $\epsilon$ at all. Substituting the summations in Eq. (D10) by integrals, one finds

$$\delta\sigma_{xx}^{7-10}(\epsilon \ll 1) = \frac{e^2}{3\pi^2}\ln\ln\frac{1}{T_{c0}\tau}+O(\epsilon), \tag{D11}$$

which just gives a temperature-independent constant. Let us stress that this constant is necessary for matching of the results in domains I and VII of Fig. 5.

#### *b. High temperatures, high fields*

In this domain of the phase diagram, we cannot omit $\ln t \gg 1$ in the denominator of Eq. (D10), but the above consideration still is applicable. As a result we get

$$\delta\sigma_{xx}^{7-10}(t \gg \max\{1,h\}) = \frac{e^2}{3\pi^2}\left(\ln\ln\frac{1}{T_{c0}\tau}-\ln\ln t\right). \tag{D12}$$

In the limit of high fields $h \gg t$

$$\delta\sigma_{xx}^{7-10}(h \gg \max\{1,t\}) = \frac{e^2}{3\pi^2}\left(\ln\ln\frac{1}{T_{c0}\tau} - \ln\ln\frac{2h}{\pi^2}\right). \tag{D13}$$

### *c. Above the line $H_{c2}(T)$ but $t \gg h_{c2}(t)$*

In this region one can restrict consideration by the LLL approximation and use the asymptotic expression (A22). In complete analogy with the case of regular part of the MT contribution one finds in the main approximation:

$$\delta\sigma_{xx}^{7-10}(t \ll 1,\widetilde{h}) = \frac{e^2}{6}\frac{t}{h - h_{c2}(t)}. \tag{D14}$$

Close to $H_{c2}(0)$, but when still $t \gg \widetilde{h}$,

$$\delta\sigma_{xx}^{7-10} = \frac{4\gamma_E e^2}{3\pi^2}\frac{t}{\widetilde{h}}. \tag{D15}$$

In the regime of QFs $t \lesssim h - h_{c2}(t)$,

$$\delta\sigma_{xx}^{7-10} = \frac{4e^2}{3\pi^2}\ln\frac{1}{\widetilde{h}} + \frac{4\gamma_E e^2}{3\pi^2}\frac{t}{\widetilde{h}(t)}. \tag{D16}$$

One can notice the tight connection between the $\delta\sigma_{xx}^{7-10}$ and $\delta\sigma_{xx}^{\mathrm{MT(reg1)}}$ contributions, it is why Eqs. (D11)–(D14) should be considered side by side with Eqs. (B8)–(B13).

## APPENDIX E: WHY DOS AND DCR CONTRIBUTIONS SHOULD BE DISTINGUISHED

While diagram 1 represents the contribution to conductivity due to the direct charge transfer by FCP, diagrams 3–10 correspond to renormalization of the one-particle conductivity in the presence of fluctuation pairing and impurity scattering. Since publication of Ref. 9, diagrams 3–10 have not been distinguished and all were attributed to the DOS renormalization. Indeed, the common element of all these diagrams,

$$\delta G_{\mathrm{fl}}(\mathbf{p},\varepsilon_n) = G_{(0)}^2(\mathbf{p},\varepsilon_n)\sum_k\int L(\mathbf{q},\Omega_k)\,\lambda^2(\mathbf{q},\varepsilon_n,\Omega_{k-n}) \times G_{(0)}(\mathbf{q}-\mathbf{p},\Omega_{k-n})\frac{d\mathbf{q}}{(2\pi)^d},$$

describes the fluctuation renormalization of the one-particle DOS:

$$\delta\nu_{\mathrm{fl}}(E) = -\frac{1}{\pi}\mathrm{Im}\int \delta G_{\mathrm{fl}}^R(\mathbf{p},E)\frac{d\mathbf{p}}{(2\pi)^d},$$

which was physically interpreted as a decrease of the Drude conductivity due to the formation of the fluctuation pseudogap at the Fermi level. Nevertheless, just above we demonstrated that close to $T_{c0}$ the contributions $\delta\sigma_{xx}^{(3-6)} \sim \ln\epsilon$ and $\delta\sigma_{xx}^{7-10} \sim \ln\ln\frac{1}{T_{c0}\tau} + O(\epsilon)$ differ considerably in their temperature dependence. Moreover, we saw that far from $T_{c0}$, the contribution to conductivity of the group of diagrams 3–6 decays as $\ln^{-2} T/T_{c0}$ [see Eq. (C9)], while $\delta\sigma_{xx}^{7-10}$ depends on temperature as a double logarithm [see Eq. (D10)]. Finally, in the regime of QFs (domain IV) the contribution $\delta\sigma_{xx}^{3-6}$, together with the AL and anomalous MT contributions, decay as $T^2$ while $\delta\sigma_{xx}^{7-10}$ in this region turns out to be almost temperature independent [see Eq. (D16)]. In view of these important differences, we determine the physical origin these two groups of diagrams more specifically.

Let us start with the Einstein relation and symbolically specify therein the fluctuation parts $\delta\nu_{\mathrm{fl}}$ and $\delta D_{\mathrm{fl}}$ of the DOS and the diffusion coefficient:

$$\sigma = \nu e^2 D \approx \sigma_0 + e^2 D_0\delta\nu_{\mathrm{fl}} + \nu_0 e^2\delta D_{\mathrm{fl}}. \tag{E1}$$

Now we consider diagrams 3–10: In diagrams 3–6 the averaging over impurities ($\langle\cdots\rangle$) of the free Green's function $G_{(0)}(\mathbf{p},\varepsilon_n)$ and the correction to the Green's function due to fluctuation pairing $\delta G_{\mathrm{fl}}(\mathbf{p},\varepsilon_n)$ is performed independently:

$$\delta\sigma_{xx}^{(3-6)} \sim \mathrm{Im}[\mathrm{Tr}\{\langle G_{(0)}(\mathbf{p},\varepsilon_n+\omega_\nu)\rangle\,\langle\delta G_{\mathrm{fl}}(\mathbf{p},\varepsilon_n)\rangle\}].$$

Such averaging results in the appearance of the decay rate $i/2\tau\,\mathrm{sgn}\varepsilon_n$ in the Green's functions and the three-leg Cooperons (3), including the entering and exiting of the propagators. Since $\delta\sigma_{xx}^{3-6}$ is defined by $\mathrm{Im}Tr\,\{\langle\delta G_{\mathrm{fl}}(\mathbf{p},\varepsilon_n)\rangle\}$ this contribution can be indeed identified with the second term in Eq. (E1).

Diagrams 9 and 10 (and analogously 7 and 8) contain the four-leg Cooperon (4) and appear due to the mutual averaging of $G_{(0)}$ and $\delta G$ over impurities:

$$\delta\sigma_{xx}^{(7-10)} \sim \mathrm{Im}[\mathrm{Tr}\{\langle G_{(0)}(\mathbf{p},\varepsilon_n)\delta G_{\mathrm{fl}}(\mathbf{p},\varepsilon_n)\rangle\}].$$

One can attribute such processes to the renormalization of the current vertex in the loop for conductivity performed in the presence of fluctuation pairing and identify $\delta\sigma_{xx}^{7-10}$ with the last term in Eq. (E1).


[1] A. I. Larkin and A. A. Varlamov, *Theory of Fluctuations in Superconductors*, OUP, Second Edition (2009).

[2] L. G. Aslamazov and A. I. Larkin, Fiz. Tverd. Tela **10**, 1104 (1968) [Sov. Solid State Phys. **10**, 875 (1968)].

[3] K. Maki, Prog. Theor. Phys. **39**, 897; **40**, 193 (1968).

[4] R. S. Thompson, Phys. Rev. B **1**, 327 (1970).

[5] L. B. Ioffe, A. I. Larkin, A. A. Varlamov, and L. Yu, Phys. Rev. B **47**, 8936 (1993).

[6] V. V. Dorin, R. A. Klemm, A. A. Varlamov, A. I. Buzdin, and D. V. Livanov, Phys. Rev. B **48**, 12591 (1993).

[7] L. G. Aslamazov and A. A. Varlamov, J. Low Temp. Phys. **38**, 223 (1980).

[8] A. I. Larkin, JETP Lett. **31**, 219 (1980).

[9] B. L. Altshuler, M. Yu. Reyzer, A. A. Varlamov, Sov. JETP **57**, 1329 (1983).

[10] J. M. B. Lopes dos Santos and E. Abrahams, Phys. Rev. B **31**, 172 (1985).

[11] I. S. Beloborodov and K. B. Efetov, Phys. Rev. Lett. B **82**, 3332 (1999).

[12] I. S. Beloborodov, K. B. Efetov, and A. I. Larkin, Phys. Rev. B **61**, 9145 (2000).

[13]M. N. Serbin, M. A. Skvortsov, A. A. Varlamov, and V. Galitski, Phys. Rev. Lett. **102**, 067001 (2009).

[14]It is worth mentioning that the contribution of diagrams 7–10, which represents the renormalization of the diffusion coefficient due to the presence of fluctuations (we call this group the DCR diagrams), was never distinguished from the DOS contributions before. It was believed that these diagrams are not singular at all close to the critical temperature, but far from the critical temperature these form together with diagrams 3–6 long, double logarithmic tails in temperature in the fluctuation conductivity.

[15]V. M. Galitski and A. I. Larkin, Phys. Rev. B **63**, 174506 (2001); Phys. Rev. Lett. **87**, 087001 (2001).

[16]A. Glatz, A. A. Varlamov, and V. M. Vinokur, Europhys. Lett. **94**, 47005 (2011).

[17]V. P. Mineev and M. Sigrist, Phys. Rev. B **63**, 172504 (2001).

[18]Numerical evaluation software and "fluctuoscopy" tools, available at [http://mti.msd.anl.gov/highlights/FC].

[19]K. Jin, B. Y. Zhu, B. X. Wu, J. Vanacken, V. V. Moshchalkov, B. Xu, L. X. Cao, X. G. Qiu, and B. R. Zhao, Phys. Rev. B **77**, 172503 (2008); B. Leridon, J. Vanacken, T. Wambecq, and V. V. Moshchalkov, *ibid.* **76**, 012503 (2007); S. Caprara, M. Grilli, B. Leridon, and J. Vanacken, *ibid.* **79**, 024506 (2009); S. Okuma, S. Shinozaki, and M. Morita, *ibid.* **63**, 054523 (2001); M. A. Paalanen, A. I. Hebard, and R. R. Ruel, Phys. Rev. Lett. **69**, 1604 (1992); T. I. Baturina, D. R. Islamov, J. Bentner, C. Strunk, M. R. Baklanov, and A. Satta, JETP Lett. **79**, 337 (2004); N. Hadacek, M. Sanquer, and J.-C. Villégier, Phys. Rev. B **69**, 024505 (2004).

[20]V. F. Gantmakher *et al.*, JETP Lett. **77**, 424 (2003).

[21]T. I. Baturina, J. Bentner, C. Strunk, M. R. Baklanov, and A. Satta, Physica B **359**, 500 (2005).

[22]L. Reggiani, R. Vaglio, and A. A. Varlamov, Phys. Rev. **44**, 9541 (1991).

[23]M. Steiner and A. Kapitulnik, Physica C **422**, 16 (2005).

[24]A. A. Abrikosov, *Fundamentals of Metal Theory* (Elsevier, Amsterdam, 1988).

[25]I. V. Lerner, A. A. Varlamov, and V. M. Vinokur, Phys. Rev. Lett. **100**, 117003 (2008).

[26]Data courtesy of M. Kartsovnik.

[27]F. Rullier-Albenque, H. Alloul, and G. Rikken, Phys. Rev. B **84**, 014522 (2011).